ABSTRACT

DI, JIN. Growth of Pancreatic Islets on Collagen Coated Textile Scaffolds. (Under the direction of Martin W. King).

Type I diabetes mellitus (TIDM) is an autoimmune disease characterized by the destruction of pancreatic β-cells in the islets of Langerhans, which results in an inability to maintain normal glucose homeostasis [1]. Current treatment options, including multiple daily insulin injections, do not provide stringent enough control of glucose levels, and ultimately lead to long term diabetes and its associated complications. The goal of this project is to develop collagen coating warp-knitted scaffold materials as extracellular matrices to support the survival and function of transplanted islets cells. The collagen-coated scaffold degrades over time, allowing for better integration into the surrounding tissue. The use of collagen also avoids the problem of specific immunogenicity and pathogen transmission. Current tissue engineering scaffolds, made by conventional scaffold fabrication techniques, are generally foams of synthetic polymers or hydrogel based. Such structures prevent cells from migrating more than 500 μm from the surface due to the lack of oxygen and nutrient supply [2]. The warp-knitting technique allows for precise control over scaffold properties, such as pore size distribution, total porosity, mechanical strength and surface chemistry.

Two thick 3-dimensional (3D) warp knitted polyester 12 and 24 gauge prototype spacer fabrics with different average pore sizes were selected as scaffold materials. In order to evaluate the suitability of their structures, a murine pancreatic β-TC6 (ATCC CRL-11506 ^{TM}) cell line, was seeded on the scaffolds at a density of 5×10^5 cells per well using 24-well

plates, cultured for 7 days and observed using scanning electron microscopy (SEM) to assess which pore size provided better adhesion and proliferation for the β-TC6 cells. DAPI staining and laser scanning confocal microscopy (LSCM) were used to evaluate the migration of the β-TC6 cells through the thickness of these two scaffolds. The SEM images showed β-TC6 cells aggregating into islet-like clusters after 7 days, with larger islet clusters on the 24 gauge scaffold material, and DAPI staining showing cells still adhering to the scaffolds after 10 days in culture.

To evaluate the effect of surface modification on cell growth, a PLA uncoated nonwoven 2-dimentional (2D) textile scaffold was compared with three different activated surfaces: i) PLA with collagen, ii) PLA with maleic acid activation + genipin and collagen immobilization, and iii) PLA with maleic acid activation + genipin treatment only. A MTT (3-(4, 5-Dimethylthiazol-2-yl)-2, 5-diphenyltetrazolium bromide, a yellow tetrazole) colorimetric assay which reduces the tetrazolium salt to formazan, using 96-well plates and a seeding density of 7,500 cells per well was used to measure the relative extent of cell viability after 7 days. From among the four scaffolds the MTT data showed that the PLA activated with maleic acid, treated with genipin and immobilized with collagen supported cell viability the best.

The 24 gauge thick warp-knitted scaffold was then coated with collagen type I to evaluate islet cell viability and functionality using an MTT assay and ELISA immunoassay respectively.

Based on these results, it was concluded that the 24 gauge scaffold structures was superior for cell growth, having an average pore size that supported islet-like aggregates *in vitro*. The 2D nonwoven PLA scaffolds activated with maleic acid, treated with genipin and then immobilized with collagen offered superior cell viability. The collagen coated 24 gauge scaffold offered superior cell viability as well as cell functionality. Further work will involve the development of surface modified 3D PLA scaffolds, which will allow single β-cells to form functional islets together with the creation of new vascular networks.

Growth of Pancreatic Islets on Collagen Coated Textile Scaffolds

by
Jin Di

A thesis submitted to the Graduate Faculty of
North Carolina State University
in partial fulfillment of the
requirements for the degree of
Master of Science

Textile Engineering

Raleigh, North Carolina

2012

APPROVED BY:

_____	_____
Dr. Martin W. King Committee Chair	Dr. David A. Gerber
_____	_____
Dr. Susan H. Bernacki	Dr. Julie Willoughby

DEDICATION

To my Beloved Family and Yuanqing Wang:

For all your infinite love and support!

BIOGRAPHY

Jin Di was born on May 30th, 1987 in Lanzhou, P. R. China. She received her B.S. in Biomedical Engineering in June 2010 from Chongqing Medical University, P. R. China. In pursuit of further studies, Jin Di joined North Carolina State University, NC, USA to start her Master of Science program in Textile Engineering in August 2010, from which she expects to graduate in October 2012. After completing her master's degree, Jin plans to join a Ph.D. program to extent her research interests in Biotextiles and Tissue Engineering.

ACKNOWLEDGMENTS

I would like to acknowledge all the people who have helped me to complete this work. First of all, I would like to express my sincere gratitude to my academic advisor Dr. Martin W. King for his patience and his generosity of sharing his vast knowledge and experience with me. Also, I am especially grateful for his support and many opportunities he has given me.

I also appreciate the support given by the other members of my advisory committee, Drs. Susan H. Bernacki, David A. Gerber and Julie Willoughby. I especially want to thank Dr. Susan H. Bernacki for her generosity of giving me access of her lab, and giving me valuable advice for planning the biological experiments and sterilizing my experimental materials. I also want to thank Dr. David A. Gerber and Lisa Samuelson from the UNC-CH Medical School for their helpful and productive collaboration.

I would like to thank all my fellow researchers, and graduate students who have helped me with my research and experiments: Valerie Knowlton, Dr. Eva Johannes, Judy Elson, Stephanie Teeter and all the lab members of Martin King's Biomedical Textiles Group.

I also would like to express my sincere appreciation to my Mom, Li Chen, my Dad, Tingzhi Di, my grandmother, Deheng Zhou, and my boyfriend Yuangqing Wang for their unconditional love, support, and encouragement throughout my entire study in the U.S.A.

Finally, I would like to acknowledge my funding sources, which included the National Textile Center (NTC), NC TraCS (UNC-Chapel Hill) and various other grants from the Collage of Textiles that provided funding during my graduate education in North Carolina State University.

TABLE OF CONTENTS

LIST OF TABLES

LIST OF FIGURES

LIST OF ABBREVIATIONS

2D	Two-dimensional
3D	Three-dimensional
E	Gauge
GB	Guide bars
BM	Basement membrane
ECM	Extracellular matrix
FBS	Fetal bovine serum
IC	Islet cell
IDDM	Insulin-dependent diabetes mellitus
T1DM	Type I diabetes mellitus
MTT	3-(4,5-Dimethylthiazol-2-yl)-2,5-diphenyltetrazolium bromide, a tetrazole
PBS	Phosphate-buffered saline
PLA	Polylactic acid
PGA	Polyglycolide
PCL	Polycaprolactone
PLCL	Poly (lactide-co-ε-caprolactone)
ELISA	Enzyme-Linked ImmunoabSorbant Assay (ELISA)
SD	Standard deviation
OD	Optical density
NGF	Nerve growth factor

IGF -I	Insulin-like growth factor-I

CHAPTER 1

GENERAL INTRODUCTION

1.1 Motivation

Every year thousands of people suffer from organ failure and tissue loss caused by disease or injury [3, 4]. Over 8 million surgical procedures are performed annually in the United States at a cost of $400 million, a large fraction of the nation's health care costs. To treat these patients with tissue loss and organ failure [5], currently there is a range of alternative therapies. They include: 1) reconstructing the damaged tissue or organ using autologous tissue from the patient, 2) transplanting compatible organs or tissues from a matched donor, 3) implanting a biocompatible mechanical device or artificial prostheses which performs the function of the lost tissue or organ function, and 4) implanting a drug delivery device [6]. Although these approaches have improved the quality of life for many patients, they are associated with various complications. For example, on receiving a donor organ, patients require life-long dependence on immunosuppressive drugs. At the same time surgical reconstruction can result in post-surgical complications, such as dehiscence, necrosis and even long-term disability [7]. Mechanical devices or artificial prostheses can be implanted or worn, and they can induce a chronic inflammatory response in the host over an extended period [6]. Drug delivery systems require repeated administration. For instance, an insulin pump for type 1 diabetes patients that malfunctions, which results in unwanted systemic disorders for patients [8]. Nowadays, transplantation of compatible tissue or organs offers the

best hope for the patients; however, the healthcare systems ability to deliver transplantation surgeries is limited due to the severe shortage of donor tissue and organs [9, 10].

Based on a recent transplant data report for 2010, the U.S. Organ Procurement and Transplantation Network (OPTN) and the Scientific Registry of Transplant Recipients (SRTR) reported that 69,954 active patients were registered on the organ transplant waiting list. However, only 29,346 transplants were performed throughout the year [11]. In addition, due to the large difference between demand and supply, about 40,600 patients died during the same year while waiting for a viable available organ. Furthermore, according to the most recent data from the OPTN website, the number of patients waiting for transplants rose to 112,645 (both active and inactive) in January 2012 [12]. Because of this critical shortage of donor organs, the field of tissue engineering has emerged with the objective of finding alternative therapies that do not rely on donor organs.

In 1993 Bob Langer broadly defined tissue engineering and regenerative medicine as "an interdisciplinary field that applied the principles of engineering and life sciences toward the development of biological substitutes that restore, maintain, or improve tissue function or a whole organ [5]." In order to deliver this therapeutic application clinically to patients, the tissue or organ is either grown *in situ* inside of the patient or alternatively, outside the patient in a bioreactor prior to transplantation. More specifically, the tissue engineering field involves a combination of the following three research strategies: 1) using isolated cells

derived either from a compatible donor or the recipient; 2) adding inductive factors, such as growth factors or collagen, to the cells; and 3) using scaffolds as cell environment matrices in order to guide the generation of the desired tissue or organ. The key to success is to expose the cells to an appropriate scaffold structure coated with collagen and/or growth factors, which facilitate the adhesion, proliferation and function of the specific cell type [13]. This field of regenerative medicine has made significant progress over the last decade, with a number of key clinical successes including the first artificial bladder [14], artificial heart valve [15], bioartificial trachea and alternative bone derivatives [16]. By reference to the literature it is apparent that various types of different tissue engineering scaffolds have been developed according to these studies [17].

Both natural and synthetic materials can be made into tissue engineering scaffolds. Collagen and alginate are two examples of commonly used natural substrates for the fabrication of scaffolds, since they contain both insoluble and soluble factors that facilitate cell attachment and promote cell differentiated functions [5]. However, there are a number of limitations to these natural material scaffolds, due to their immunogenicity, pathogenicity, and their limited ability to control their mechanical properties, purity, degradation rate, consistency and reliability, and specific structural requirements, such as total porosity, average pore size and pore size distribution [17, 18, 19].

To solve these problems, synthetic biomaterials are being considered and applied to fabricate tissue-engineering scaffolds. They permit more precise design and control over scaffold properties, both mechanical and chemical. They also avoid the inherent problems of immunogenicity and pathogenicity [20]. Examples of currently used biodegradable synthetic polymers include, polylactic acid (PLA), polyglycolic acid (PGA), and polylactic-co-glycolic acid (PLGA), which have been approved by the Food and Drug Administration (FDA) for use in a range of biomaterial devices [21]. Resorption results from the hydrolysis process, which occurs after implantation *in vivo* or on exposure to moisture. The by-products of hydrolysis are non-toxic and can be easily excreted by the human body [22]. While one obvious deficiency of a synthetic material scaffold is its lack of critical biomacromolecules and growth factors that provide an active cell growth environment. In order to effectively direct cell growth on these scaffolds, they must be modified with key elements that allow them to resemble native ECM [23]. There are three kinds of desirable ECM components, which can either be incorporated into the synthetic scaffold or coated onto the scaffold's surface. The first are the structural proteins, such as collagen and elastin, which function like a connective web to provide elasticity to the tissue. The second are the adhesive proteins, such as laminin and fibronectin, which function as binding sites for cell adhesion, and the third kind are the basement membrane proteins, such as collagen type I, which function like molecular glue that promotes a confluent monolayer of epithelial and endothelial tissues. [24]. One thing that needs to be stressed is that the basement membrane is critical in the design of scaffolds for regenerative medicine, since the formation of new blood vessels

requires endothelial cells to grow directly on the basement membrane. And for successful regenerative therapies the artificial scaffold and newly regenerated tissues need to be well vascularized in order to function *in vivo* after transplantation [25].

The use of appropriate biomaterials that contribute to the restoration of islet cell function is one of the most promising cell-based therapies. In fact islet cell transplantation offers a hope for patients who have type 1 diabetes mellitus. However, current methods have not achieved the anticipated goal of long-term insulin independence. Difficulties have been reported when the transplanted islets are either rejected by the immune system after a few months or they lose function due to an insufficient oxygen and/or nutrition supply at the transplantation site [26]. Recent research results from using an animal T1DM model have shown that by selecting the appropriate biodegradable scaffolds, the islet cells' function and survivability has been greatly improved [27]. The scaffolds serve as a platform to provide a controllable microenvironment and improve islet cell attachment and proliferation.

1.2 Goals and Objectives

The overall goal of the work presented in this thesis is first to research the hypothesis that a 3D warp-knitted scaffold may be used as an inductive platform to promote the survival and function of transplanted islet cells. Second, it also evaluates three different surface modification methods that are applied to 2D nonwoven scaffolds made from PLA fibers to determine the most effective way to enhance islet cell attachment.

To better understand these goals, three specific objectives have been developed as follows:

1) To compare the structure and cell culture performance of two thick 3D warp-knitted spacer fabrics that have different values for total porosity and average pore size. The 12 gauge knitted scaffold had a total porosity of 86.25 ± 0.02% and average pore sizes of 0.07 ± 0.03 mm compare to the 24 gauge knitted scaffold with a slight lower total porosity of 85.63 ± 0.02% and an average pore size of 0.04 ± 0.01.
    1.1 To discuss the general requirements for tissue engineering scaffolds for beta-TC-6 islet cell culture, such as average pore size, total porosity and the desired culturing conditions based on findings of the literature review.
    1.2 To create a practical plan for in vitro beta-TC-6 islet cell seeding and to assess the cell proliferation on these two scaffolds by different evaluation methods, such as SEM and LSCM.
2) To evaluate the islet cell adhesion performance on the surface of a series of four 2D PLA nonwoven scaffolds that had received four different surface activation and modification treatments.
    1.1 To compare the surface modification methods by measuring beta-TC-6 islet cell viability using MTT assay after 7 days of cell culture.
3) To study the effect of collagen coating of the thick 24 gauge 3D warp-knitted spacer fabric PET scaffold, this was tested in Objective 1, to give superior cell attachment.

1.1 To analyze the surface characteristics after collagen coating using TOF-SIMS technology and the contact angle method.

1.2 To assess the biocompatibility of the collagen coated thick 24 gauge PET scaffold by culturing beta-TC-6 islet cells for 3, 7 and 10 days. The assessments included the conduction MTT assay for cell viability, SEM and LSCM for cell adhesion and migration at different time points, and the ELISA immunoassay to measure islet cell function in terms of insulin production.

1.3 Significance of this Study

Currently, there are a growing number of diabetic patients who need to control their unstable blood sugar levels with injection of exogenous insulin. The surgical alternative of transplanting human islets or pancreases has so far demonstrated limited success. It is therefore important to find an effective clinical therapy that relies on the concepts of regenerative medicine to tissue engineer viable and functional islet populations that will provide normal glucose homeostasis for this growing cohort of patients. It is significant not only to improve the quality of life for these patients who suffer from this debilitating disease, but also to reduce the financial impact on the whole of society, which has to provide healthcare for these patients, and treat their disease and concomitant diabetic comobities, which cost billions of dollars each year.

By studying the design, surface chemistry and structure of engineered biomaterial scaffolds so as to evaluate the molecular factors, which support and promote proliferation, migration and function of transplanted islets, we may be able to improve the success rate of islet transplantation surgery. The experimental results from this study have the potential to advance this field by identifying the types of scaffold structures and the preferred ECM component molecules, which promote the growth, and function of transplanted islets.

CHAPTER 2

REVIEW OF LITERATURE

In this literature review, we introduce the range of different types of tissue engineering scaffolds that have been used to regenerate viable pancreatic tissue *ex vivo*. The various types of polymeric biomaterials are reviewed together with their chemical, mechanical and biological properties. This is followed by a review of the different approaches to scaffold design using fibers and non-fibrous materials, their structures and performance. An important and related topic concerns their biocompatibility and how cell adhesion and proliferation can be improved by certain surface modification techniques. Clearly to achieve these objectives it is necessary to involve an interdisciplinary team of researchers in the fields of surgery, medicine, biology, mechanical and electrical engineering, chemistry, material, fiber and polymer science.

In this review of the literature we focus on the treatment of Type I diabetes and the need for transplantation of the pancreas and/or pancreatic islets.

Type 1 diabetes mellitus (T1DM) is an autoimmune disease, which leads to a loss of the insulin-secreting β-cell in the islets of Langerhans and the subsequent abnormalities of glucose homeostasis depending on the patients' daily activities. T1DM has become a

significant burden to both patients and society. Although the precise pathogenesis of T1DM is still unknown, scientists have found in genetically susceptible individuals, some environment factors that can trigger the onset of this disease, which is a particular concern for children and young adults. Current treatment methods, such as daily injections of exogenous insulin to maintain the desired blood sugar level, are difficult to achieve in children and adolescents. This has led to new therapeutic approaches, for instance, pancreas and islet transplantation procedures, which have now been performed for more than 10 years. However, in order to maintain the functionality of the transplanted organ or tissue, patients are required to take immunosuppressive drugs over the long term. In addition, the number of available organs is quite limited. For these two main reasons the widespread use of organ transplantation therapy is limited. Under such circumstances, regenerative medicine and the use of tissue engineering scaffolds has emerged as an attractive therapy by offering a 3D microenvironment for the culture of isolated islets so as to promote their viability, proliferation and function in a diabetic recipient. Many types of scaffold materials and structures have been studied with the objective of optimizing those critical factors that will achieve a long-term therapy for T1DM.

2.1 Type I Diabetes Mellitus

Approximately 10% of the U.S. population is affected by autoimmune diseases. Among these diseases there is a type called organ specific autoimmune diseases, in which the targeted organ can be impaired, damaged and even destroyed by an aggressive immune response [28].

Type 1 diabetes mellitus (T1DM), also known as insulin dependent diabetes mellitus (IDDM) or juvenile onset diabetes, is one of such organ specific autoimmune diseases and is characterized by losing the ability to maintain normal glucose homeostasis. This is due to the insulin-secreting beta cells in the islets of Langerhans in the pancreas being completely destroyed by the targeted immune response [28, 29, 30]. As one of the major metabolic diseases, T1DM occurs most frequently among Europeans and is currently the most common chronic disease threatening children [31]. In the U.S. it is estimated that over 1.5 million people have T1DM [32], and this number continues to grow by 10,000 to 15,000 new diagnosed cases annually. Moreover, this phenomenon is worldwide [32, 33, 34, 35]. Although the exact pathogenesis of T1DM is still a mystery, some factors are known to trigger the onset of T1DM, such as environmental and genetic factors and immunopathogensis, which have been demonstrated experimentally by several researchers and have been used to predict the incidence of T1DM with a fair degree of certainty [36, 37].

2.1.1. Pathogenesis

Recent research articles agree that the following three aspects, genetic factors, environment factors and immunopathogenesis, all contribute to the onset of T1DM. And these three factors have also been used to predict diabetes in individuals. From genetic studies, the frequency of T1DM is higher than the general population in descendants of diabetic parents, and their siblings. Chromosome 6 in the human leukocyte (HLA) region is the most essential gene to determine T1DM susceptibility [28, 38]. While the possibilities of developing T1DM

is highly dominated by genetic factors, stimulating the autoimmune process cannot be triggered without environmental factors. These factors included hygiene status, viral infection, diet and toxins [39, 40, 41]. In an individual's early childhood, if the child is infected by the virus Coxsackie B, rubella or mumps, they can be directly affected by the destruction of β-cells resulting in the rapid onset of T1DM [42]. From this point of view the hygiene status of children at an early age is important. Certain studies have found that the risk of developing T1DM actually decreases if one has had an infection in one's childhood, since this can enable the immune system to develop a regular protective mechanism that lowers the risk of autoimmunity on further exposure. So ironically today's cleaner environment is a likely factor that triggers T1DM [43]. Factors related to diet have been investigated a lot recently. Consuming too much sugar and fat, early exposure to cereal products and a lack of balanced nutrition are all linked to an increased risk of developing T1DM, especially for these individuals who are genetically susceptible [44, 45].

2.1.2. Current Clinical Treatment

Patients with T1DM suffer life-threatening diabetic ketoacidosis (DKA). This happens because of insufficient insulin production, which causes a metabolic deficiency of decomposing ketone bodies into fatty acids, and leads to an increased release of glucose by the liver (a process that is normally suppressed by insulin) [46, 47]. The patient with T1DM feels fatigued and has a tendency to rapidly lose weight, experiences dehydration and compensatory thirst. The patient with T1DM also suffers from blood acidosis, the smell of

ketones in their breath, hyperglycemia and cerebral edema. This can lead to confusion, recurrent vomiting, susceptibility towards infection and a number of clinical complications that can result in early death [48].

The majority of T1DM treatments available today are multiple daily subcutaneous injections of exogenous insulin. This therapy is administered following blood glucose monitoring (normal range 80 ~ 150 mg/dL), so as to supply the body with sufficient insulin to control glucose hemostasis [49, 50]. To better assist diabetic patients to control their unstable blood sugar levels after meals and overnight, various devices have been invented, such as the insulin pump implanted under skin, which can provide the desired level of insulin in response to a blood sugar level sensor [51]. However, these devices are expensive, subject to mechanical and electronic failure, exposing patients to hypoglycemia, which is not well tolerated. While it is true that the usage of insulin can help diabetic patients avoid acute hyperglycemia, this intensive insulin injection therapy has not resulted in a decrease in T1DM and its associated comobidities. It has only delayed their onset; it has not eliminated them! These complications not only decreased the quality of life of diabetic patients but also impose a heavy burden of cost on both the patients' family and society [52, 53].

2.1.2.1. Organ Transplantation (Pancreas or Islets)

The first attempt to transplant a whole pancreas in to a diabetic patient was made in 1966 by a team of Dr.Kelly, Hillehei, Merked, Inezuki and Goetz. But this trial did not succeed due to

a lack of immunosuppressive drugs following surgery [54, 55]. In the late 1970's, new discoveries were made on improving pancreas transplantation procedures, selecting compatible donor organs and administering immunosuppressive therapy after surgery [56, 57, 59]. Soon successful clinical cases increased up to 80%. However, even today there are still risks associated with pancreatic transplantation. The requirement of taking immunosuppressive drugs for life limit these operations to only end-stage diabetic patients [60]. Although whole pancreas transplantation works well for patients with T1DM, the number available of donor organs is far too small compared to the large number of diabetic patients who need them [61]. In response to this severe organ shortage an alternative innovation and less invasive surgical approach of islet transplantation was born [62, 63].

In late 1990s, clinicians established a series of standardized procedures for pancreas procurement, islet isolation and immunosuppressive drug regimens. For those cases where, T1DM patients were able to accept islet transplantation, they achieved stable insulin independence. However, in order to transplant a sufficient number of islets into one recipient, islets had to be isolated from 2-4 donor organs, which severely limited the potential for this type of therapy [64, 65, 66]. Clinical follow up studies have reported that up to 80% of T1DM patients who receive islets transplantation surgery were insulin independent after 1 year, but according to a later report, only 7% of these patients still remain insulin independent after 5 years [67, 68]. Recent reports provide evidence that only a fraction of normal β-cells is needed to maintain normal blood sugar levels, and suggest that cultured

islets from a single donor can survive and function well post-implantation. These reports provide encouraging signs that islet transplantation can be used in the future to achieve temporary and long-term insulin independence for T1DM patients [69, 70, 71]. However, in order to achieve long-term islet transplantation success, a number of issues such as islet isolation procedures, cell cultivation and the transplantation site need to be investigated further [72, 73]. Multiple sites have been reported as suitable locations for islet transplantation, such as the liver, spleen, kidney capsule and omentum [74]. Among them, the liver is widely accepted as a feasible site for transplantation and is currently the option of choice [75, 76].

2.1.3. Economic View

With the increasing number of individuals with T1DM, the health care cost for treatment of this disease and its secondary comobitidies places a significant burden on our society [77, 78]. The overall estimated cost related to T1DM in the U.S. in 2010 was $184 billion, including hospital inpatient care, medication, surgical supplies, and treatment of complications of T1DM [79]. According to these facts and figures, the average yearly medical cost of patients with T1DM is about 2 - 3 times higher than for people without T1DM. This fact alone imposes a significant financial burden on the patient's family [80. 81]. This is particularly true for a child with T1DM who requires a lifetime of continual blood sugar monitoring and insulin injections, which generates healthcare costs more than twice that of a healthy child. For these reasons, there is significant interest in finding

alternatives ways to treat T1DM so as to better match normal insulin secretion levels and reduce the cost of T1DM treatment [81]. Pancreas and islet transplantations are both promising new treatments under investigation.

2.2 Biology of the Pancreas and Islets

The main disease associated with a malfunctioning pancreas is diabetes mellitus, a disease in which patients are unable to control the level of sugar (glucose) in their bloodstream due to their inability to produce insulin on demand. Other diseases affecting the pancreas include exocrine pancreatic insufficiency, when the required digestive enzymes are not generated and the patient is unable to digest food properly. Then there is pancreatitis or inflammation of the pancreas, which may be caused by various conditions such as cystic fibrosis and alcoholism; and pancreatic cancer, which is one of the most lethal cancers with a 5-year survival rate of less than 5% [81]. The use of transplanted islets for the treatment of diabetes is hindered by the difficulty in obtaining sufficient numbers of beta cells. Islets constitute only between 1% and 2% of pancreatic tissue [82]. Since a large number of pure pancreatic islets being required for successful clinical and experimental transplantation, it is usually necessary to combine islets isolated from two to three donors in order to make successfully transplant a single T1DM patient. Consequently the relatively low number of available donors is a major limiting factor to the widespread use of islet cell transplantation. With the objective of identifying an effective strategy to culture sufficient numbers of viable and functioning islet

cells *in vitro* so as to satisfy the increasing demand for islet transplantation, we need to understand the biology of both the pancreas and islet cells.

2.2.1 Biology of the Pancreas

The pancreas is a pear-shaped gland (Fig.2.1) [85] located in the abdomen between the stomach and the spine. It is about six inches in length and is composed of two major components [83]. The exocrine component is made up of ducts and acini (small sacs at the end of the ducts), which produce specific enzymes that are released into the small intestine to help the body break down and digest food, particularly fats. The endocrine component of the pancreas is made up of specialized cells clustered together in islands within the organ, called islets of Langerhans. These cells produce specific hormones, with the most important one being insulin, a substance that helps control the amount of sugar in the blood [84].

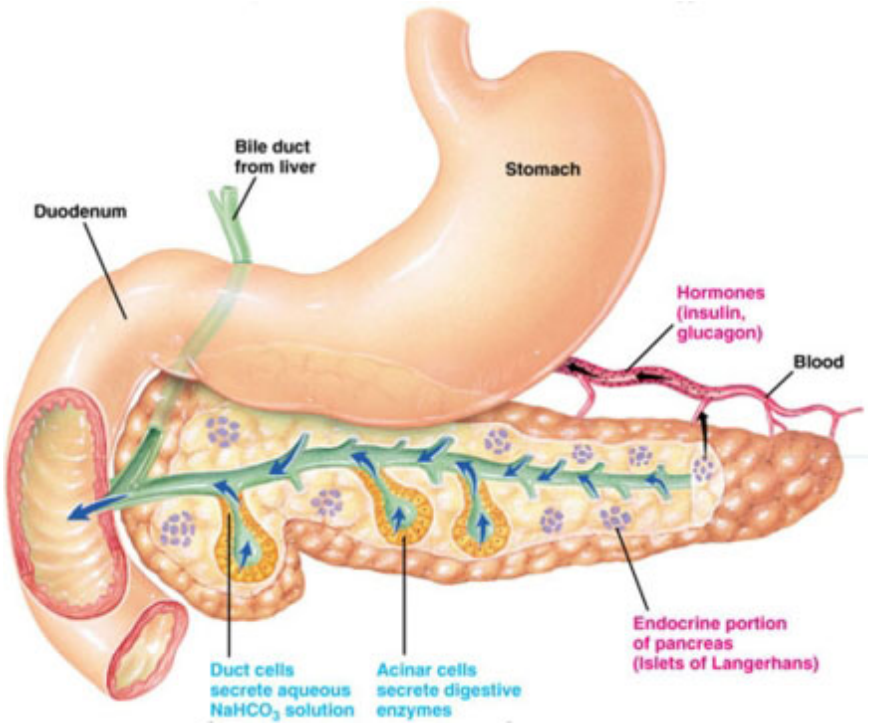

Figure 2. 1 . The Anatomical Structure of the Pancreas [85].

2.2.2 Biology of Islet Cells

Normally, the weight of the human pancreas's is about 50~75 grams [86]. The islets of Langerhans (Fig.2.2) [87] constitute approximately 1 to 2% of the mass of the pancreas, but they receive 5-15% of the pancreatic blood supply because they need to serve the serum glucose level and then adjust the amount of insulin secretion so as to maintain normalglycemia [88]. There are about one million islets in a healthy adult human pancreas, which are distributed throughout the organ; their combined mass is 1.0 to 1.5 grams. Islets are clusters of endocrine cells that are distributed throughout the pancreas. The hormones

produced in the islets of Langerhans are secreted directly into the blood by five major cell types. Alpha cells (15-20% of total Islet cells) produce glucagon. Beta cells (65-80%) produce insulin and amylin, and occupy the central core of each islet, with the other types of cells surrounding it. Delta cells (3-10%) produce somatostatin, pancreatic polypeptide (PP) (3-5%) cells produce pancreatic polypeptide, and epsilon cells (<1%) produce ghrelin. The islets can influence and control each other through paracrine and autocrine communication. The beta cells are coupled electrically to other beta cells but not to the other cell types. The paracrine feedback system of the islets of Langerhans has the following function. Insulin activates beta cells and inhibits alpha cells. Glucagon activates alpha cells, beta cells and also delta cells. Somatostain inhibits alpha cells and beta cells [89].

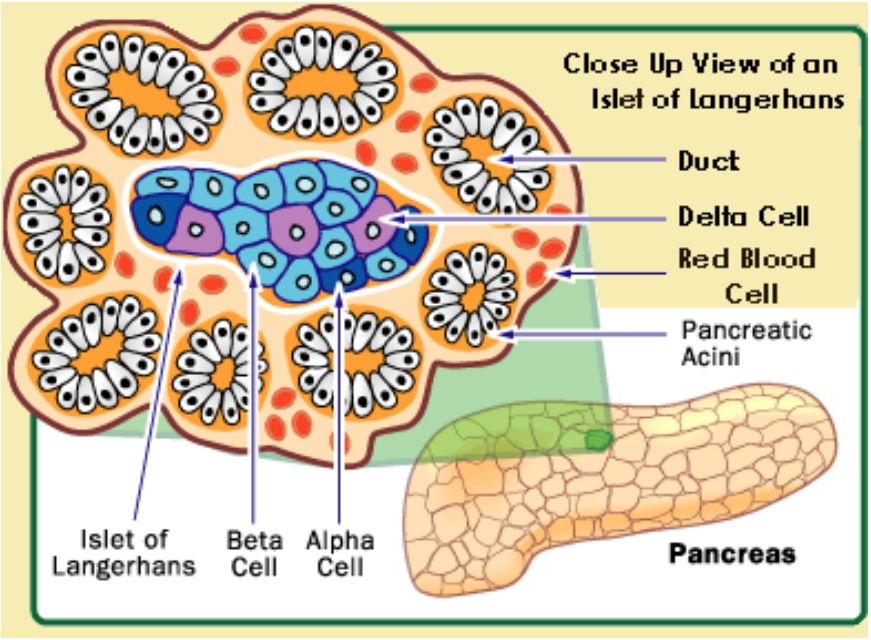

Figure 2. 2 . Islet Cells of Langerhans [87].

The procedure of islet isolation invariably results in vascular disruption which is a critical factor in β-cell survival, because angiogenesis and the formation of new vascular connections normally requires 7-14 days after transplantation [90]. Because during this period the rich β-cells in the central region tend to experience necrosis combined with apoptosis, prior revascularization is essential to enhance islet cells survival and function and to achieve the goal of insulin independence. Also, a number of growth factors have been investigated to promote insulin secretion and proliferation: 1) Hepatocyte growth factor, which functions to increase insulin secretion and the proliferation of islets [91]. 2) NGF functions in both *in vitro* and *in vivo* conditions to improve β-cells survival [92]. 3) IGF-1, this factor shares a similar molecular structure to insulin, and has proven to increase islet graft survival [93]. 4) Exendin-4 (E4), betacellulin (BTC) and activin A all play an important role in promoting β-cell regeneration and promoting cell differentiation in adults [94]. Although we have listed here several of the known growth factors, there are still many factors whose role remains unknown. So while it is well established that growth factors do improve β-cell population, viability, it is evident that growth factors are only one part of the *in vitro* and *in vivo* environment. The role of the extracellular microenvironment is equally important.

2.2.3 ECM Microenvironment for Islet Cells

The extracellular matrix (ECM) is an essential component for any specific type of tissue since it is the fundamental substance to supply nutrition, anchor cells and regulate cell

behavior. Thus, understanding the ECM components of a tissue is a prerequisite to the design of functional and effective tissue engineering scaffolds [95-99]. Pancreatic islets are surrounded *in vivo* by the ECM which not only provides structural anchorage for the islets but also mediates signals that are crucial to the survival of the islets. Enzymatic digestion of the pancreas during islet isolation results in a separation from the ECM which has been shown to induce islet cell death. Furthermore, islets require the ECM for optimal functionality. Thus, the re-establishment of islet-ECM contact with the use of a biodegradable scaffold may contribute to increased islet survival and better preservation of the islet mass post transplantation, hence offering longer-term graft function. The islets-ECM microenvironment is composed of basement membranes (BMs), which mainly consist of collagen IV, laminins, and fibronectin. The BMs provide structural support, a network of blood vessels, and they regulate islet cell behavior by providing several molecular cues, as shown in Fig.2.3 [100-105]. Based on previous findings obtained from mice islet studies, collagen IV is responsible for providing structural support to anchor the cells, while laminins combined with integrins located on the surfaces of islet and endothelial cells control intercellular signaling which leads to islet cell proliferation, migration, differentiation and finally apoptosis [105, 106]. Islets cultured on tissue engineering scaffolds containing ECM components have successfully demonstrated improved islet survival *in vitro* [107-110].

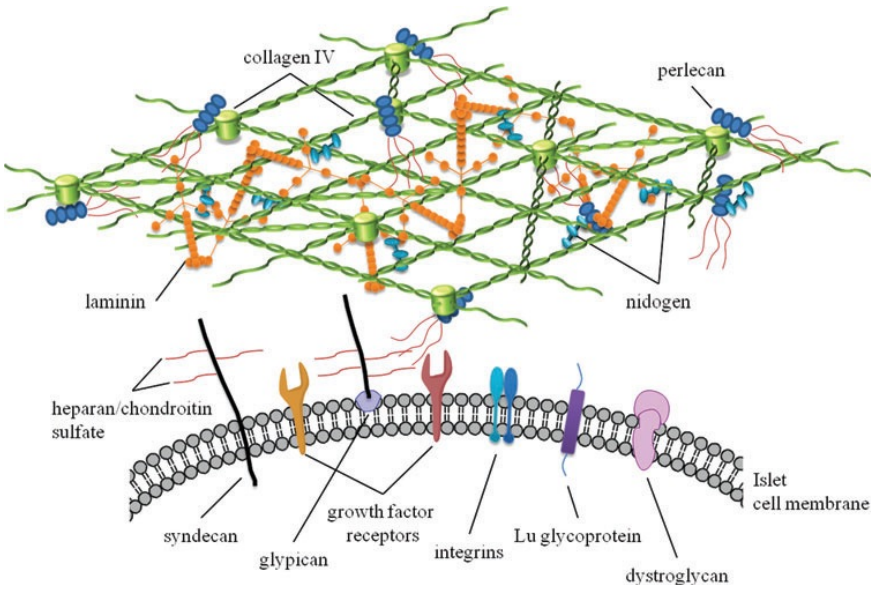

Figure 2. 3 . Major Components of Islet Extracellular Matrix (ECM) and Potential Cell Surface Receptors [99].

2.3 Tissue Engineering and Regenerative Medicine Therapies

Regenerative medicine is a very broad subject. It requires contributions from many fields, including cell biology, biomedical engineering, material science, computer engineering and clinical medicine. Generally it is defined as "the engineering and growth of functional biological substitutes in vitro and/or the stimulus to the regeneration and remodeling of tissues in vivo for the purpose of repairing, replacing, maintaining, or enhancing tissue and organ functions [111]." Currently, regenerative medicine has three main areas of application. 1) Cell therapy, which uses living cells to restore, maintain and enhance the function of a specific organ or tissue without scaffolds or encapsulation. Typical examples are the

transplantation of bone marrow, and pancreatic islets transplantation for the treatment of T1DM, and hepatocyte transplantation to cure liver disease [112, 113]. 2) Tissue engineering (Fig.2.4) requires the aid of scaffolds as physical support structures which also regulate molecular cues that are grafted on the scaffolds to stimulate cell growth and function. This approach is obviously more complex and expensive than cell therapy, and examples include engineered skin, artificial bone, cartilage substitutes and cornea reconstruction [114-116] 3) Bioartificial organs, which extend the concept of tissue engineering by combining several different types of tissues so as to design and fabricate a functioning implantable organ with the main goal of supporting the patients failing organ, such as the liver or kidney. Preliminary clinical trials of bioartificial livers and implantable artificial renal dialysis devices indicate positive effects for patients with both acute and chronic liver failure and patients suffering from renal failure [117, 118].

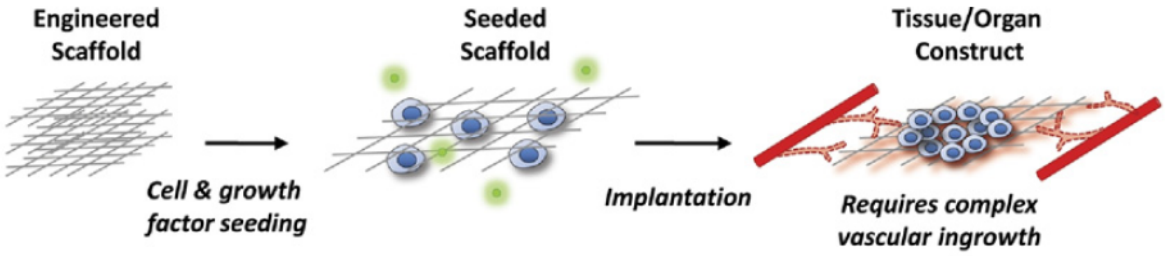

Figure 2. 4 . Tissue Engineering Method. Seeding of cells and/or growth factors on scaffolds and subsequently implanting the viable composite construct into the host [111].

2.3.1 Current Clinical Experience

Islet transplantation has proven to be an effective treatment for a select population of individuals with T1DM, but many obstacles remain before it can be applied more widely. The need for a large number of islets to achieve euglycemia, and the progressive deterioration in islet function over time, represent two significant barriers. The cause of these problems is not yet fully understood because allo- or autoimmune-mediated damage to the islets cannot fully account for these issues. The transplantation of islets into the liver may contribute to islet dysfunction and necrosis loss due to an impaired blood supply. Thus, one priority in the field of islet transplantation is to develop an extrahepatic site. The renal subcapsular space is a well-established site for islet transplantation in rodent models, but anatomic differences have precluded the use of this site in nonhuman primates and humans. The peritoneal cavity and omentum have been suggested as alternative sites for islet transplantation as these sites are safe in humans. In one particular clinical study, intraperitoneal fat was selected as the site for islet transplantation. In fact the findings clearly demonstrate a beneficial effect of the polymer scaffold on islet function by using a polymer scaffold to support cell viability following transplantation into abdominal fat [119, 120]. In previous animal studies transplanting islets in to the peritoneal cavity of rodents has produced inconclusive results. In the present study we use a microporous polymer scaffold with the goal of enhancing integration of transplanted islets into the host tissue.

2.3.2 Various Biomaterials Used for Islet Cell Scaffolds

Islet transplantation has been reported as an ideal therapy for the treatment of T1DM. The islets normally are cultured for a period of time *in vitro* to achieve the desired population for transplantation. However, islet viability and function are limited by using a 2D culture plate, and for this reason a 3D *in vitro* culture environment is necessary. In the last few years, much progress has been made in this field, including the use of hydrogel encapsulation, fibrin glue, and various polymeric biomaterial scaffolds made of PLA, PGA, PCL and PLCL [121, 122].

The desired properties of the scaffold are biocompatibility and degradation into non-toxic by-products within the desired time frame so as to not provoke any adverse tissue response. The rate of biodegradability of the scaffold depends mainly on the selection of the polymer [123]. Currently 3D scaffolds made from either natural or synthetic biomaterials, serve as a primary research tool to mimic the essential features of the natural islets' ECM. Their role is to support cell adhesion and provide a source of nutrition and growth factors by immobilizing ECM components on the surface. In this way they promote islet cell attachment, growth and proliferation on the surface of the scaffold [124]. The key properties of currently used polymers are summarized in Table 2.1 [123-127]. Poly(lactic acid) (PLA) is widely used in tissue engineering because this polymer is biodegradable and has been approved by the US Food and Drug Administration for clinical use in a variety of applications. Due to the presence of an extra methyl group in lactic acid, PLA is more hydrophobic than PGA and less soluble in aqueous systems [126]. Polycaprolactone (PCL) is also an aliphatic polyester

that has been investigated intensively as a biomaterial. PCL has a longer degradation period compared to PGA and PLA. Hence it is more suitable for long term degradation implants or devices. Poly (lactide-co-ε-caprolactone) (PLCL) is a random copolymer synthesized from both lactic and caprolactone. Since it is less crystalline, it has a lower modulus and high elongation at break, which makes this aliphatic polyester copolymer more suitable for soft tissue applications such as skin, liver and pancreas. Porous PLCL materials have also been prepared for controlled drug release experiments using freeze-drying or salt-leaching techniques to generate the pores [127].

Table 2. 1- Properties of Biodegradable Polymers

Polymer	Thermal/ Mechanical Properties					Degradation (months)
	T_m (°C)	T_g (°C)	Modulus (Gpa)	Tensile Strength (MPa)	Elongation (%)	
PLA	173 - 178	60 - 65	2 - 5	55 - 82 (900 - fiber)	5 - 10	>24
PGA	225 - 230	35 - 40	7.0	>70 (890- fiber)	15 - 20	6 - 12
PCL	58 - 63	-65	20 - 35	22 - 38	300 - 500	>24
PLCL	90 - 120	-17	23 - 25	12 (film)	600 (fiber)	6 - 8

2.3.2.1 Fiber-based Tissue Engineering Scaffolds

In order to design more complex constructs, fibers can be formed in to three-dimensional (3D) structures such as knitted, braided and woven fabrics, and nonwoven webs. The

orientation of the fibers in these structures may range from being highly oriented to completely random. In fact the final density and orientation of the textile structure will affect the behavior of the fibers in the different layers. For example, woven fabrics have a more stable and less porous structure than the other types of textile structures. One of their major disadvantages is that they can unravel at the edges when they are cut squarely or obliquely for implantation.

Warp knit structures on the other hand, have an inherent ability to resist raveling when cut and are flexible and porous, but some of their flexibility is reduced when additional yarns are used to interlock the loops and obtain a more stable structure. The spaces between the yarns, which loop around each other, make them porous and help fluid transport during the cell culture process. Nonwoven webs can have a wide range of porosities. If the web is laid down in a random process their isotropic structure provides good mechanical and thermal stability in all directions. If a carded or oriented web is prepared then multiple layers are cross-lapped at different orientations before bonding, like plywood, so as to give a uniform and isotropic mechanical performance.

After the scaffolds have been fabricated, sterilization is also an important subsequent step of tissue engineering applications. Due to the fact that polymers generally have lower thermal and chemical stability than metallic and ceramic materials, they are also more difficult to sterilize using conventional techniques. In addition, the polymers used for pancreatic islet

cell scaffolds are biodegradable, which requires sterilization methods that do not interfere with the material's bulk properties. The most common commercial sterilization techniques are dry heat, moist heat or autoclaving, gamma or electron beam radiation and ethylene oxide gas [123]. The biodegradable scaffolds used for islet transplantation in previous experimental studies were sterilized using alcohol and ultra-violet light [127]. The scaffolds were soaked in 70% ethanol about 30 min. However, for cell culture the alcohol needs to be completely removed before the cells are seeded. Therefore several washes with a phosphate buffered saline were necessary followed by drying on a sterile bench and exposure to ultraviolet light for 1 hour [123, 128]. Before the islets cells were seeded, the scaffolds were washed three times in islet growth medium and soaked in the medium for 30 min. However, these experimental procedures are complicated and include uncontrolled humid conditions that may have damaged the scaffolds. In this study, we used a standard exposure to ethylene oxide gas to sterilize our scaffolds and reduce the potential damage to a minimum.

2.3.3 Surface Modification and Collagen Immobilization on Scaffolds

In any implantable medical device good biocompatibility is required so that the device can function in subcutaneous tissue. The implantable constructs for culturing pancreatic islet cells are composites of biological material (islets of Langerhans) and a supporting polymeric scaffold. The successful implantation of this polymeric scaffold depends on good biocompatibility with the biologic tissue and the formation or angiogenesis of a viable vasculature for reliable blood supply. Surface modification of the polymeric scaffold is

important to improve its biocompatibility. Often the goal of the engraftment is hindered by the normal tissue inflammatory reaction to the implant device, which must support the growth and function of the islets while maintaining the graft in an immunologically privileged state. Viability of the graft requires nutrient and oxygen supply, and metabolite removal. In general, synthetic polymers themselves do not generate sufficient angiogenic signals, and so one approach to improved vascularization is to modify the chemistry and or physical characteristics of the implants' surface. The chemical composition, reactive groups, and leachable component, such as monomers, inhibitors and catalysts, determine whether a given polymer is likely to behave as a biocompatible and nontoxic implant. The surface polarity and hydrophobicity is another important characteristic which influences protein adsorption and subsequent steps involving cell interactions. It is well known that cell adhesion, spreading and proliferation are strongly dependent on providing a hydrophilic solid surface [128].

Among the many different techniques for surface modification, there are three methods to modify the scaffold's surface. 1) Non-thermal plasma technology produces a high concentration of energetic and active species including ions and free radicals at room temperature which can physically ablate and chemically modify the scaffold surface, making it more hydrophilic or hydrophobic depending on the conditions (Fig.2.5) [129]. 2) Free radical graft polymerization technique is an effective way to chemically modify a scaffold's surface by growing and crosslinking of polymer chains on or near the surface. Our laboratory

has recently demonstrated how this approach can be used to activate a synthetic PLA polymer surface by the formation of an interpenetrating polymer network. 3) The use of a living free radical graft polymerization technique, differs from the above two methods, because it does not break or crosslink any chain during the reaction, while minimizing bimolecular termination and prolonging the life of the living free radical [130, 136].

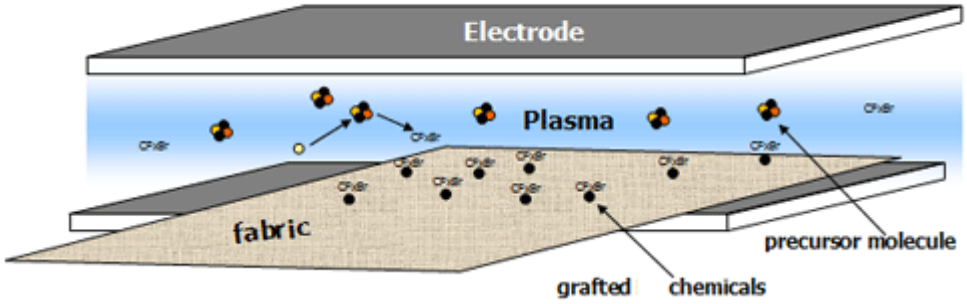

Figure 2. 5. Schematic of Atmospheric Pressure Plasma Reactor [129].

As we have discussed above, collagen is the most abundant and important macromolecule in the ECM. As well as being biodegradable and non-immunogenic, it improves islet cell attachment. Various methods have been described to physically immobilize collagen to a scaffold's surface, including microwave energy, UV radiation and thermal drying treatments. However, the degree of crosslinking is unpredictable. In response to this, chemical crosslinking agents have been used, such as aldehydes, polyepoxys and diols. However most of them are cytotoxic [131]. So to solve this problem in this study, we have used genipin, which is a natural crosslinking agent or spacer molecule (Fig.2.6) obtained from the fruit of the Genipa Americana plant [132, 133, 136].

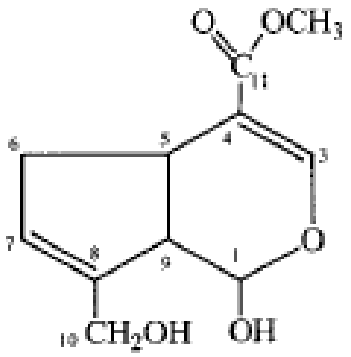

Figure 2. 6. Chemical Structure of Genipin [132].

Chapter 3 Experimental

3.1 Introduction

Islet transplantation offers the potential to successfully treat patients with T1DM. However, the shortage of organ donors and the immunologic issues associated with islet transplantation have limited widespread application of this therapy. In addition to these two issues, the disruption of a critical vascular tube and its accompanying extracellular matrix have impaired the engraftment and function of transplanted islets during the isolation process. These interactions play important roles in regulating many aspects of islet cells physiology, such as viability, proliferation, functionality and insulin secretion. Thus, the reconstruction of an extracellular matrix becomes necessary following islet isolation. In this chapter, tissue-engineering scaffolds are described as a platform for islet cells by providing a 3D matrix which supports islet cells attachment, proliferation and function. The materials and methods used throughout the experiments are described in detail in this chapter. The whole study is composed of three parts. To begin with in the first part, two types of porous scaffold were fabricated from PET yarns using a 12 gauge (12E6GBXII) and a 24 gauge (24E6GBXII) warp knitting machine. These two different structures were included in order to find out which one would be better at supporting islet cell attachment and proliferation. Then, after determining the preferred structure, it was necessary to modify the scaffold's surface so as to improve its rate of resorption and biocompatibility. So in the second part, 2D scaffolds

fabricated from PLA nonwoven fabric were activated and then treated by three different surface modification techniques (two involving collagen and one with genipin alone), and evaluated to determine which technique was most appropriate for the culture of beta-cells. In the third and last part we extended the work of the previous two sections. Based on the results from the first two parts of the study, the third part was designed to evaluate the 24 gauge warp knitted 3D PET scaffold coated with type I collagen. Previously collagen has been shown to support a variety of cell types, including mouse liver and pancreatic islet cells. This previous series of experiments has demonstrated that collagen promotes islet cell viability, proliferation, cytocompatibility and a positive response to glucose stimulation. These studies provide some insight into how our 3D scaffolds after coating with type I collagen may enhance the viability and functionality of cultured islet cells *in vitro* and further their usage both as basic research tools and as therapeutic agents in the clinic.

3.2 Materials and Methods

3.2.1 Scaffold Structure Evaluation

Poly(ethylene terephthalate) (PET), which has good mechanical stability and biocompatibility, is not bioresorbable. The 150 denier 48 filament textured polyester (PET) yarn was obtained from Unifi Inc. Yadkinville, NC, USA, and was used to fabricate warp knitted 3D spacer fabric samples for this study. The structural and mechanical properties of the PET yarn as provided by the manufacture are listed in Table 3.1.

Table 3. 1 - PET Yarn Properties

Properties	**Cross-section**	**Breaking tenacity**	**Elongation at break**	**Shrinkage**	**Density**	**Twist direction**
PET yarn	Round	4.7 gpd	20.4%	14.8% (180F)	1.38 (g/cm^3)	S

The PET yarns were knitted at NCSU on a double needle bed narrow width (26 inches) tricot Karl Mayer DR 10 warp knitting machine with two interchangeable sets of needles, 12 gauge and 24 gauge. The two types of knitted samples were identified as 12E6GB and 24E6GB, according to the gauge (E), needles per inch, and the number of guide bars (GB), as shown in Figs. 3.1 and 3.2.

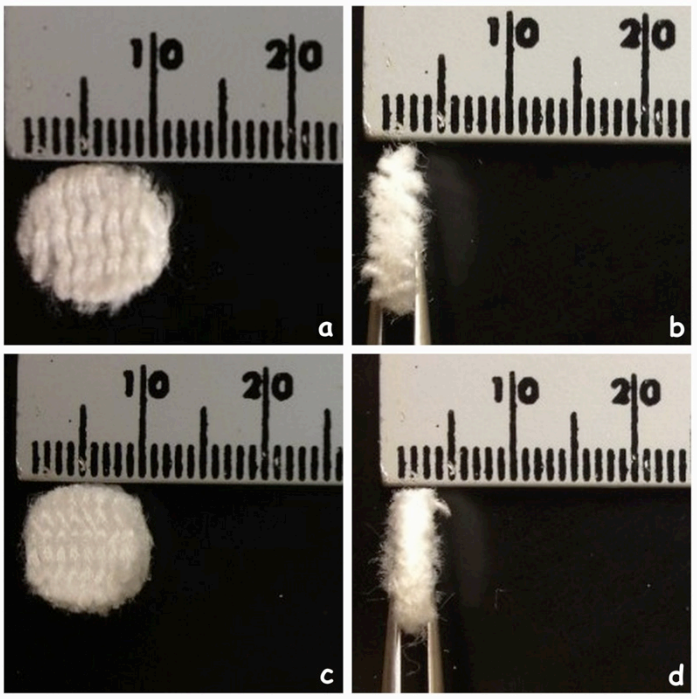

Figure 3. 1. Circular Specimens Cut from PET Warp Knitted Spacer Fabric Scaffold Samples (Diameter 10 mm). (a) Face and (b) Cross-section of 12 Gauge 6 Guide Bar sample with XII Spacer Yarn Structure (12E6GBXII). (c) Face and (d) Cross-section of 24 Gauge 6 Guide Bar Sample with XII Spacer Yarn Structure (24E6GBXII).

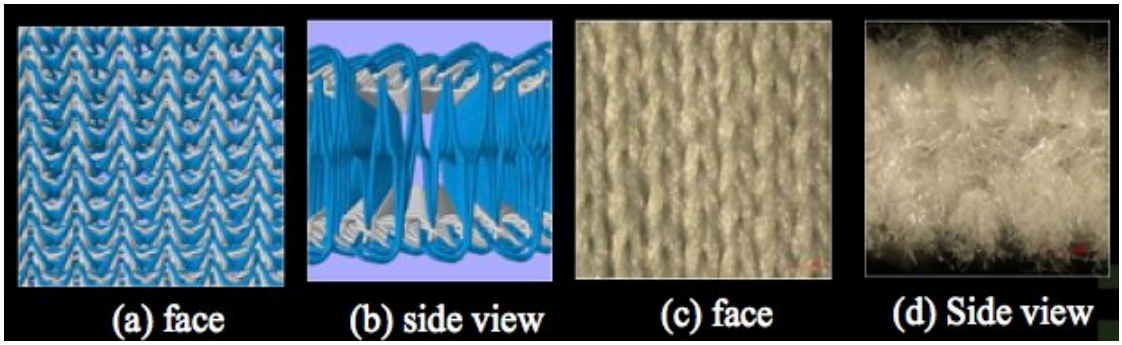

Figure 3. 2. Top Face and Cross-sectional Views of 3D PET Warp Knitted Spacer Fabric Scaffold Samples. (a) and (b) computer software generated images, (c) and (d) optical microscopic images (Magnification 50x). [137]

The samples were thoroughly cleaned by scouring to remove dirt, oil and other impurities with 1% Triton ^{TM} X - 100 detergent for 10 min at 60 ° C followed by rinsing with deionized water three times and then drying in a vacuum oven at 50 ° C overnight. When dry the samples were cut into 10 mm diameter discs with a punch.

After the samples were cut into 10 mm disks, the scaffold specimens were immersed in 70% EtOH for 15 min to remove any oil during the punching process. This was followed by 3 washes in PBS, allowing the scaffolds to dry overnight in a vented hood and then sterilizing them in ethylene oxide gas overnight in a sealed container.

Beta-TC-6 insulinoma cells were acquired from American Type Culture Collection (ATCC, VA, USA). They are an insulin-secreting cell line derived from transgenic mice expressing the large T-antigen of simian virus 40 (S40) in pancreatic beta-cells. They were expanded in

ATCC complete growth medium (15% heat-inactivated fetal bovine serum, 1% Penicillin and 84% Dulbecco's Modified Eagle's Medium) and incubated with 5% CO_2 at 37 °C for up to 7 days in order to generate enough cells. The medium was replaced every 3 days. Before seeding, the culture medium was removed and discarded. The cells were briefly rinsed with PBS to remove all traces of serum. Then 3.0 ml trypsin solution were added to one T-75 flask and the flask was returned to the incubator for 3 min. After 3 min the flask was taken out and the cells observed under an inverted microscope until the cell layer had dispersed. Six ml complete growth medium were added to stop the reaction and the cells were aspirated by pipet. The cell suspension was centrifuged at 1100 rpm for 2 min so the cells could form a pellet. The supernatant was carefully removed and an appropriate amount of complete growth medium was added to dilute the cells to 0.5 x 10^6 cells/ml. The scaffolds, which had previously been put into a 24-well plate, were seeded by adding 1 ml cell suspension to each well. The scaffolds in the 24-well plate with a density of half million cells/well were cultured for 7 days with the medium being replaced every 2 days. At the seventh day the scaffolds were harvested by washing 3 times in PBS to remove any traces of serum. They were then fixed by immersing in 3ml of 2% gluaraldehyde in PBS (Fixatives, VT, USA) and keeping them at 2-8 °C for at least 24 hours. Then after drying they were mounted for viewing under SEM. In order to visualize the cells migrating through the thickness of the scaffolds, the cross-section of the scaffolds was viewed under laser scanning confocal microscopy (LSCM). The same cell seeding method as described above was used to culture the cells for 5 and 10 days. The scaffolds were then fixed by immersing them in 3ml of 2% gluaraldehyde in PBS

(Fixatives, VT, USA) and keeping them at room temperature for 20 min before DAPI staining.

To coat the PET spacer fabric samples directly with collagen without any activation the scaffolds were immersed in 0.01% Type I collagen solution and the protein was allowed to penetrate and bond overnight at 2-8 °C. The next day the excess fluid was removed, and the scaffolds were washed three times with PBS to remove any unbound protein before drying in a vented hood at room temperature.

3.2.1.1 Scanning Electron Microscope (SEM)

Scanning electron microscopy (SEM) was harnessed in order to see how the beta-TC-6 cells attached themselves to the spacer fabric scaffolds, and also to determine if there was a significant difference in cell attachment between the 12 gauge and 24 gauge scaffolds. Specimens were viewed in a JEOL JSM-5900LV scanning electron microscope (JEOL USA, Inc. Peabody, MA, USA) under high vacuum conditions with an accelerating voltage of 20 kV.

The cells cultured on the scaffolds were harvested after 7 days. They were fixed using a standard protocol. A monobasic phosphate buffer (PBS) was prepared at a pH of 7.2 – 7.4. The scaffolds were fixed in 3% glutaradehyde solution (Ladd research) in PBS, and then stored at 4 °C for at least 24 hrs before post-fixation procedures, which were carried out

using a standard protocol in the Department of Biology SEM laboratory within the College of Agriculture. The scaffold specimens were mounted on aluminum stubs using conductive carbon tape and sputter-coated with gold-palladium before storing in a desiccator. The JEOL software was used to align the specimens and capture the images taken at random on the top and bottom surfaces at a range of different magnifications.

3.2.1.2 Laser Scanning Confocal Microscope (LSCM)

It is important to know if the cells migrated through the thickness of the 3D spacer fabric scaffolds. To answer this question, laser scanning confocal microscopy (LSCM) was used to visualize the extent of cell migration throughout the thickness of the scaffolds. A Zeiss Model LSM 710 laser scanning confocal microscope (Carl Zeiss MicroImaging, NY, USA) was employed. This type of microscope is capable of generating a series of 2D cross-sectional images (spatial resolution: 512 x 512 pixels) from the top surface to the bottom of the whole scaffold since the scan head attached to the Zeiss Axio Observe Z1 inverted microscope had a motorized x, y and z stage. Zen software (Carl Zeiss MicroImaging, NY, USA) was used to reconstruct 3D images from the series of 2D captured images and to perform the analysis.

The cells were seeded on scaffolds and cultured for 5 and 10 days. Prior to viewing at each time point, the scaffolds were removed from the medium, followed by three washes in PBS buffer to remove any traces of cell culture medium. In order to expose the cross-section of

the scaffolds to LSCM imaging, each scaffold was then cut in half by a sharp surgical blade. Then DAPI stain was used to identify and determine the number of live cells.

3.2.2 Surface Modification Evaluation

A sample of polylactic acid (PLA) 2D nonwoven web was obtained from Ahlstrom Nonwovens LLC (Windsor Locks, CT). The basis weight of the web was 20 gsm, and it was bonded by needle punching. A mixture of D- and L- mixed isomer resin (D < 2%) was used to spin the fibers, which were supplied by Nature Works LLC. This nonwoven textile structure was referred to as two dimensional (2D) because the web of PLA fibers was laid down in the x, y plane without orienting any significant numbers of fibers in the thickness direction (3 plane). Upon arrival in our laboratory the nonwoven sample was thoroughly cleaned by scouring in 1 g/L soda ash and 1 g/L nonionic surfactant (Triton x100) at 60 °C for 30 min, followed by three rinses with deionized water to remove any oil and other impurities. After scouring, the samples were dried overnight in a vacuum oven, and then stored in sealed paper envelopes in a desiccator.

Because the PLA polymer does not have any reactive groups in its structure to graft collagen or other protein to its surface, it is necessary to functionalize the fiber surface. In our laboratory, we used maleic acid as the monomer to impart functionality to the surfaces of the PLA fibers. The monomer was grafted onto the surfaces by a plasma initiated polymerization technique. The activated PLA sample was then reacted with genipin (Wako Chemicals,

Fisher Scientific) by immersing the activated nonwoven samples in genipin solution for about 6 hour at room temperature. Genipin is a naturally occurring cross linker, which acts like a spacer molecular to immobilize matrix protein and improve the cytocompatibility of the scaffold. Type I Collagen (MP Biomaterials LLC) derived from calfskin was immobilized by immersing the genipin treated PLA samples in a collagen/glacial acetic acid solution for 24 hrs at 2 – 8 °C. Then the samples were sterilized in ethylene oxide gas overnight, followed by three washes in PBS so as to achieve the desired pH 7.2 – 7.4 for cell culturing.

For the cell studies, Beta-TC-6 insulinoma cells acquired from the American Type Culture Collection (ATCC, VA, USA) were expanded in ATCC complete growth medium (15% heat-inactivated fetal bovine serum, 1% Penicillin and 84% Dulbecco's Modified Eagle's Medium), incubated with 5% CO_2 at 37 °C and prepared for seeding on the scaffolds. Six 10 mm diameter PLA scaffold specimens were prepared from each treated and untreated PLA sample (see Fig. 3.3) and placed in a 24-well plate.

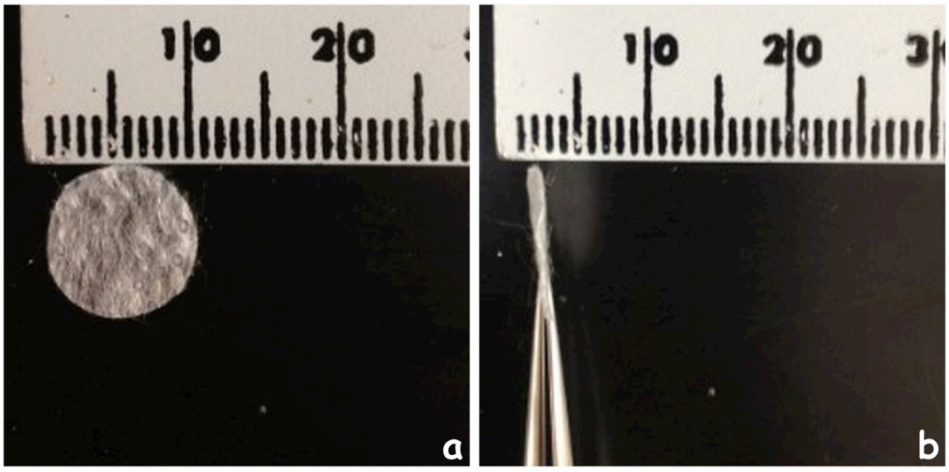

Figure 3. 3. PLA 2D Nonwoven Sample as Received (diameter 10 mm). (a) Surface of the PLA sample (b) Cross-section of the PLA sample.

Three kinds of the treated PLA samples were included in this cell study. They included:

a) The collagen coated PLA sample without surface activation.

b) The PLA sample which had been functionalized by maleic acid, treated by genipin and exposed to collagen immobilization.

c) The PLA sample which had been grafted with maleic acid and genipin, but without any collagen immobilization.

The expanded cells were harvested and then seeded onto the scaffolds with a seeding density of 7,500 cells/well and allowed to grow onto the scaffolds for 3 and 7 days in order to evaluate cell viability. At the same time, scaffold specimens without cells, blank wells and wells with cells only served as negative controls and were processed in the same manner as

the cell cultured specimens. At each time point, the scaffolds were analyzed by the MTT assay for cell viability.

3.2.2.1 MTT Cell Viability Assay

The cell viability test was performed by incubating beta-TC-6 islet cells seeded scaffolds with 3-(4,5-dimethylthiazol-2yl)-2,5-diphenyl tetrazolium bromide (MTT, Sigma-Aldrich Co. LLC, MO, USA), which is reduced to an insoluble purple formazan product by the mitochondria of living cells.

A MTT solution was freshly prepared by dissolving the MTT powder in phosphate buffer solution (PBS) to achieve a concentration of 5 mg/ml solution. It was then filter sterilized using a 0.22 μm filter (Millipore, USA). At each time point, the scaffolds were transferred to a new 24-well plate, followed by three washes in PBS. One ml complete cell culturing medium (without phenol red) was added to each well together with 50 μL of prepared MTT solution prior to incubation for 4 hours at 37 °C/ 5% CO_2. After 4 hrs, the supernatant was carefully removed without disturbing the formed formazan. One ml of dimethyl sulfoxide (DMSO) was then added to dissolve the formazan followed by incubation for 30 min at 37 °C/ 5% CO_2 to allow the formazan to dissolve. After 30 min, the solution in each of the 24 wells was then transferred into four separate wells (250 μL/ well) in a new 96 well plate for absorbance measurements, which were read by a microplate reader (Genios, Tecan US Inc., Durham, NC, USA) at 540 nm.

3.2.3 Evaluation of Collagen Coated 3D Scaffold (24 Gauge)

The presence of Type I collagen on PLA 2D nonwoven tissue engineering scaffolds has been shown to improve the viability and proliferation of beta-TC-6 islet cells in previous *in vitro* studies [54]. Also the previous results obtained from the 3D scaffold structure evaluation in this study showed that the 24 gauge scaffolds supported beta-TC-6 islet cell attachment better than the 12 gauge scaffolds, since the 24 gauge spacer fabric had a smaller average pore size. However, the effect on cell growth of combining a 3D scaffold structure with PLA surface modification is not well understood. In this section of experiments, the cell viability, proliferation, migration through the scaffold, and response to glucose stimuli were assessed directly by culturing beta-TC-6 islet cells on the 3D 24 gauge PET scaffolds coated with Type I collagen. Additionally, cell morphology was assessed by a scanning electron microscope at 3, 7 and 10 days following cell seeding on the collagen coated scaffolds.

3.2.3.1 Material

The 3D PET scaffolds used in this section of experiments were the same PET 24 gauge scaffolds, that had been used previously and described in Section 3.2.1 (see Figures 3.1, 3.2 and 3.4).

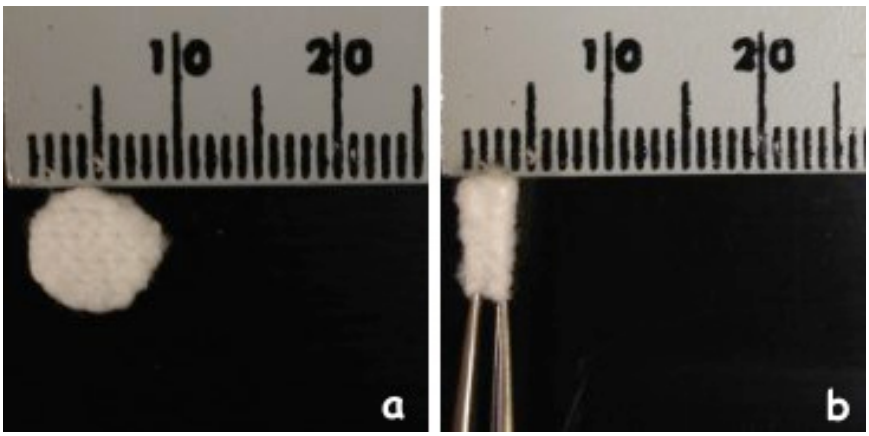

Figure 3. 4. PET Warp Knitted Spacer Fabric Scaffold Samples with 24 Gauge, 6 Guide Bar and XII spacer Yarn Structure (Diameter 10 mm) with 24 gauge, 6 Guide Bars, XII Spacer Yarn Structure. (a) Surface appearance. (b) Cross-sectional view.

3.2.3.2 Methods

3.2.3.2.1 Time-of-Flight Secondary Ion Mass Spectrometry (TOF-SIMS)

An experimental method for the identification and possible relative quantification of collagen on the PET 3D spacer fabric, face and back as well as on the cross-sectional views has been developed. The TOF-SIMS technique which is a highly sensitive surface analytical method with high spatial and mass resolution [134], has been used in this study for the acquisition of elemental and molecular information from the scaffolds within the top, middle and bottom 10 to 20 Å. The principle behind this technique is to use a finely focused, pulsed primary ion beam to scan across the surface of the sample and the secondary ions emitted at each irradiated point or pixel are extracted and fed into a time of flight mass spectrometer where

their mass is filtered and the number of positive and negative ions for each mass number are counted. For example, an image with sub micrometer (< 0.3 μm) spatial resolution can be acquired with a full mass spectrum for each pixel. In this study, the TOF-SIMS analysis was done using a TOF-SIMS V (ION TOF, Inc. Chestnut Ridge, NY) instrument equipped with a Bi_n^{m+} (n = 1 - 5, *m* = 1, 2) liquid metal ion gun. The vacuum system of this instrument was composed of two parts, a load lock for sample loading and an analysis chamber, which were separated by a gate valve. In order to avoid sample contamination, the analysis chamber pressure was always maintained below 5.0 x 10^{-9} mbar. In order to achieve high mass resolution with a 128 by 128 pixel spectrum of a 100 μm by 100 μm area a Bi^+ primary ion beam was used. However for a 256 by 256 pixel image of a 200 μm by 200 μm area a Bi_3^+ primary ion beam was used instead. To avoid charge buildup on the analyzed sample surface, an electron gun was used to achieve a primary ion accumulation during spectral image acquisition of less than 1 x 10^{13} ions/cm^2 (within the static SIMS regime) After acquiring an initial signal, the secondary ions were extracted and fed into a TOF mass spectrometer with post acceleration in order to improve the detection sensitivity. The positive secondary ion mass spectra obtained were calibrated by the H^+, C^+, CH^+, CH_2^+, $C_2H_5^+$. $C_3H_7^+$ ions, and at the same time, the negative secondary ion mass spectra were calibrated in terms of the C^-, O^-, OH^- and C_n^- ions. After calibration and signal smoothing a mass resolution of approximately 5000m/Dm was obtained at 29AMU.

In this study, the distribution of collagen on the 3D PET scaffolds was obtained by comparing the two-dimensional mapping of the TOF-SIMS signal distribution for collagen in green and comparing it to that for polyester (PET) in red. The homogeneity on the treated scaffolds was assessed by evaluating the uniformity of the red or green color on the face and back surfaces of the cross-sectional views.

3.2.3.2.2 Contact Angle

Wettability refers to the phenomenon that describes how a liquid behaves once it is deposited on a solid substrate. High wettability reflects its ability to spread and interact with the substrate, and subsequently to support cell adhesion and proliferation, which is one of the more important properties of tissue engineering scaffolds. Measurement of the contact angle is one way to determine a textile scaffold's surface wettability before and after surface modification. It is often used to provide information about the hydrophilic or hydrophobic character of a fabric, and it can also reflect the surface energy of a fabric. See Fig. 3.5.

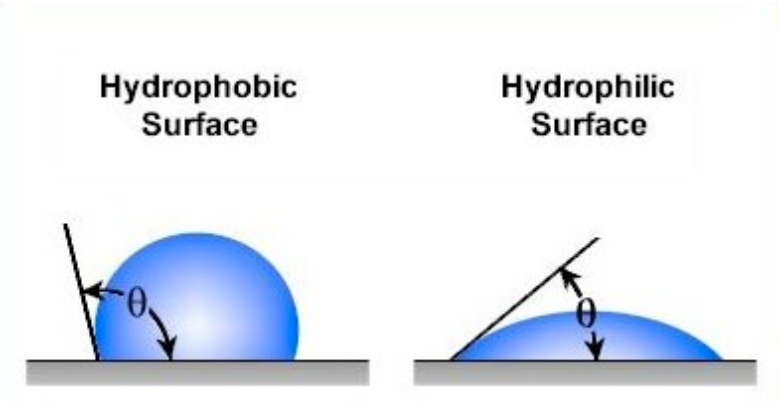

Figure 3. 5. Contact Angle Results of Hydrophobic and Hydrophilic Surfaces.

Contact angle (Θ) is the angle formed between the liquid-vapor and liquid-solid interfaces at the solid-liquid-vapor phase contact point. To simplify this definition, the contact angle is measured between the tangent of the drop and the solid interface as shown in Figure 3.6.

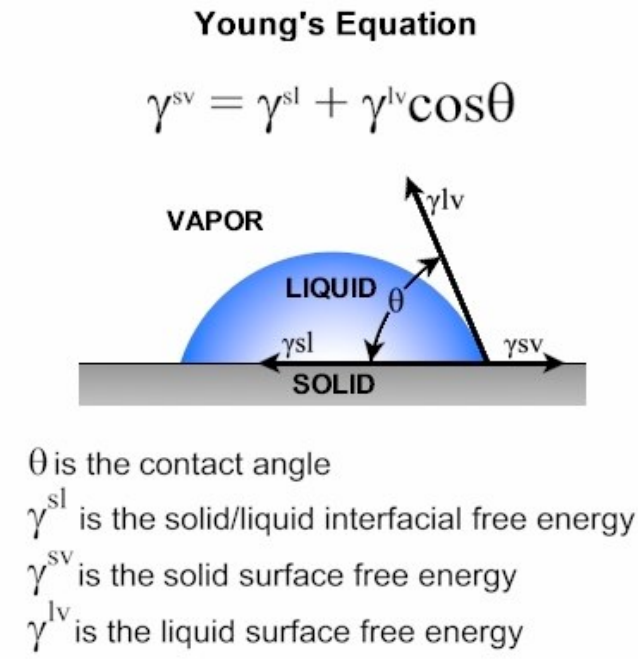

Figure 3. 6. Measurement of Contact Angle

The calculation of contact angle measurements relies on using Young's equation as shown in Figure 3.6. The Young's equation assumes a smooth, rigid and homogeneous surface and the use of an inert liquid droplet.

Because textile surface have a fibrous and rough structure, the base line and construction points at the intersection of the 3 phases have to be estimated. This leads to inherent variability in the measurements. In addition, the size of the open pores in the textile surface will cause some variation in the case of droplet absorption into the textile. In this study, the

contact angle measurements were performed on an OCA 20 Model DataPhysics video based optical contact angle measuring system with SCA 20 software. The instrument was also equipped with a CCD video camera (resolution 768 x 576 pixels), an electronic dosing system, an electrically driven sample stage and an electronic syringe unit for delivery of the droplet, as shown in Figure 3.7.

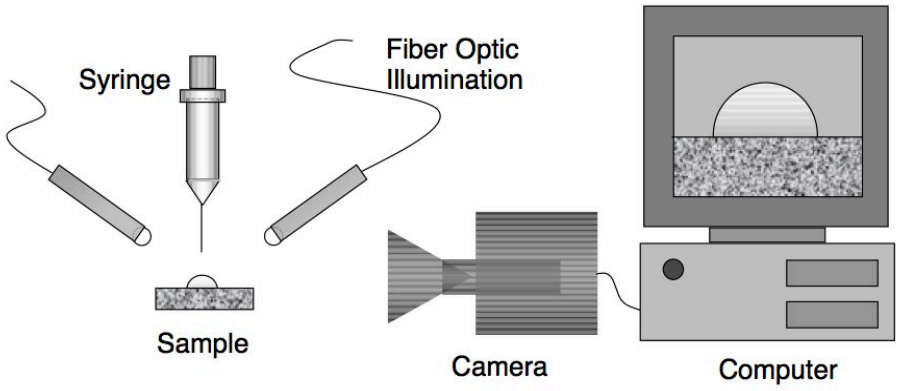

Figure 3. 7. Experimental Set Up for Measuring Contact Angle.

The treated and untreated 3D 24 gauge knitted PET scaffold fabrics were cut into rectangular shaped specimens measuring 1 cm x 4 cm in size and they were taped down onto the specimen stage before testing. The static contact angle was measured by the sessile drop test of 5 µl of PBS from a 500 µl syringe dropped at 10 µl/min volume rate. Before the test the syringe was filled with sterile PBS and attached to the electronic dosing system. The SCA 20 software then adjusted the stage to acquire a clear vision of the needle and the specimen. The PBS droplets were then dropped onto the scaffold's surface one at a time, and images were taken at 0, 30s, 60s and 90s with the SCA software following the droplet's arrival time. To

obtain an average contact angle, the same procedure was repeated at five different locations across the specimen's surface.

3.2.3.2.3 Cell Viability Assay (MTT)

Cell viability was determined using the 3-(4,5-Dimethylthiazol-2-yl)-2,5-diphenyltertrazolium bromide (MTT) test after 0, 3, 7 and 10 days of culture. The samples that were collagen coated and those without collagen were sterilized by ethylene oxide overnight and washed three times with PBS before introducing the cells and medium. At each time point, the scaffolds were removed and placed in a clean 24-well plate before addition of the MTT solution. The MTT stock solution was made by directly adding MTT powder to sterilized PBS at a concentration of 5 mg/mL, and then filtering it through a 0.22 μm filter to remove any impurities. The MTT solution was added in an amount that is 15% of the culture volume and the cultures were incubated for 4 hours. After 4 hours, the cultures were carefully removed without disturbing the formed formazan crystals and 1mL DMSO was added to dissolve them. The 24-well plates were placed in an orbital shaker operating at 60 cycles / min for 15 min to promote the dissolution of the formazan crystals. The absorbance rate was measured at a wavelength of 540 nm. A reproducible linear calibration curve of absorbance rate vs. cell numbers was obtained. The linear correlation was found experimentally to equal: $y = 0.4998x - 0.4722$ ($R^2 = 0.99862$).

3.2.3.2.4 Cell Morphology on Scaffold Surface (SEM)

Scanning electron microscope was employed to investigate the morphology and attachment of cells to the scaffolds, with and without collagen coating after 3, 7 and 10 days of cell culture. After each time point, the specimens were first fixed in 4% glutaraldehyde and 0.01M phosphate buffer solution (PBS) for 24 hr. They were then dehydrated gradually by immersing the specimens in the following series of aqueous ethanol solutions: 30%, 50%, 70%, 90% and 3 x 100% ethanol each for 30 min. After this process, the specimens were exposed to liquid CO_2 for 10 min at equilibrium (1350 psi, 40 ° C) using a critical point dryer (Tousimis Samdri-795, Rockville, MD) before mounting them on aluminum stubs using conductive carbon tape. The specimens were then coated with gold/palladium using a Hummer ^{TM} 6.2 Sputter Coating System (Anatech, CA, USA) to achieve a coating around 100 Å thick. Images were obtained using a JEOL JSM 5900-LV scanning electron microscope and an accelerating voltage of 20 kV.

3.2.3.2.5 Cell Migration throughout the 3D Scaffold (LSCM)

To visualize the cell migration throughout the thickness of the scaffolds, a laser scanning confocal microscope (Zeiss LSCM 710, Carl Zeiss MicroImaging, NY, USA) was used with a 10 X 0.45 NA dry Plan Apochromat objective. Before acquiring any images, the specimens were fixed with 2% glutaraldehyde in PBS buffer at room temperature for 30 min, and then stained with propidium iodide solution (PI, Sigma, USA) for 5 min at room temperature. The

PI solution was prepared freshly by adding 100 μL of 2 mg/mL PI stock solution to 10 mL PBS buffer. The scan head was attached to a Zeiss Axio Observer Z1 inverted microscope with motorized x, y and z stage. Excitation was achieved with a 405 nm diode and the emission absorbance was in the range of 409 to 507 nm during the image capturing process. Sections of the confocal 2D sliced images were generated from the top through to the bottom in 100 μm slices for each specimen. The spatial resolution of the images was 512 x 512 pixels. ZEN software (Carl Zeiss MicroImaging, NY, USA) was used for the 3D image reconstruction.

3.2.3.2.6 Detection of Islet Cell Function (ELISA Immunoassay)

Beta-TC-6 islet cells (n = 5 x 10^5 cells/ well) were seeded onto the scaffolds. Both specimens coated with and without collagen were placed in a 24-well plate prior to cell culturing for 0, 3, 7 and 10 days for islet cell function using the ELISA assay. At each time point, the specimens were washed three times in PBS buffer, and then one group was stimulated in serum and glucose free DMEM culture solution for low glucose (0 mMg/mL), while the other group was stimulated by the same culture solution but with a high glucose solution (100 mMg/mL). Cultured cells were incubated for 30 min, 1 hr, 2 hr, and 4 hr at 37 ° C in the presence of 5% CO_2 for detection of insulin in the culture solution. The supernatants collected from the specimens (Fig. 3.8) were evaluated by an insulin (mouse) ELISA (Enzyme-Linked ImmunoabSorbant Assay) immunoassay (ALPCO ™, NH, USA) for the quantitative determination of insulin in mouse serum and plasma (Fig. 3.9). The ALPCO

insulin (Mouse) ELISA is a two parts enzyme immunoassay. The mouse insulin antibodies were first immobilized on the 96-well micro plate as a solid phase before the test. Then the samples, standards, controls were added to the specific wells with the conjugate. Fig. 3.10 shows the ELISA plate will arrangement for end color development. After incubation on a microplate shaker (Fisher Vortex Genie 2, PA, USA), which was operated at 700-900 rpm at room temperature for 2 hours, the microplate was washed 6 times with PBS buffer to remove unbounded conjugate. The 3,3′,5,5′-Tetramethylbenzidine (TMB) Substrate was added to each well, followed by another 15 min incubation on a microplate shaker at 700-900 rpm at room temperature. After 15 min incubation, a blue color was produced by the TMB substrate reacting with bound conjugate, and the stop solution was added to stop the reaction and turn the blue color to yellow. The optical density values were measured by a microplate reader (BioTech, VT, USA) at 450 nm with a reference wavelength of 620-650 nm. The amount of insulin in the sample was directly proportional to the optical density of the yellow color generated. The insulin release index was calculated as the ratio of the high glucose value divided by the low glucose value.

		1	2	3	4	5	6	7	8	9	10	11	12
30 min L	A	MO1	MO9	CO17	CO25	TG33	TG41	C1-49	C1-57	C2-65	C2-73	C3-81	C3-89
1 hr L	B	MO2	MO10	CO18	CO26	TG34	TG41	C1-50	C1-58	C2-66	C2-74	C3-82	C3-90
2 hr L	C	MO3	MO11	CO19	CO27	TG35	TG43	C1-51	C1-59	C2-67	C2-75	C3-83	C3-91
4 hr L	D	MO4	MO12	CO20	CO28	TG36	TG44	C1-52	C1-60	C2-68	C2-76	C3-84	C3-92
30 min H	E	MO5	MO13	CO21	CO29	TG37	TG45	C1-53	C1-61	C2-69	C2-77	C3-85	C3-93
1 hr H	F	MO6	MO14	CO22	CO30	TG38	TG46	C1-54	C1-62	C2-70	C2-78	C3-86	C3-94
2 hr H	G	MO7	MO15	CO23	CO31	TG39	TG47	C1-55	C1-63	C2-71	C2-79	C3-87	C3-95
4 hr H	H	MO8	MO16	CO24	CO32	TG40	TG48	C1-56	C1-64	C2-72	C2-80	C3-88	C3-96

Figure 3. 8. Specimen Supernatant Collecting Map. (L: Low 0 mM Glucose/mL; H: High 100 mM Glucose/mL; MO: Medium Only; CO: Cell Only; TG: Collagen Coated Scaffold with cells; C1: without collagen coated scaffold with cells; C2: collagen coated scaffold without cells; C3: without collagen coated scaffold without cells)

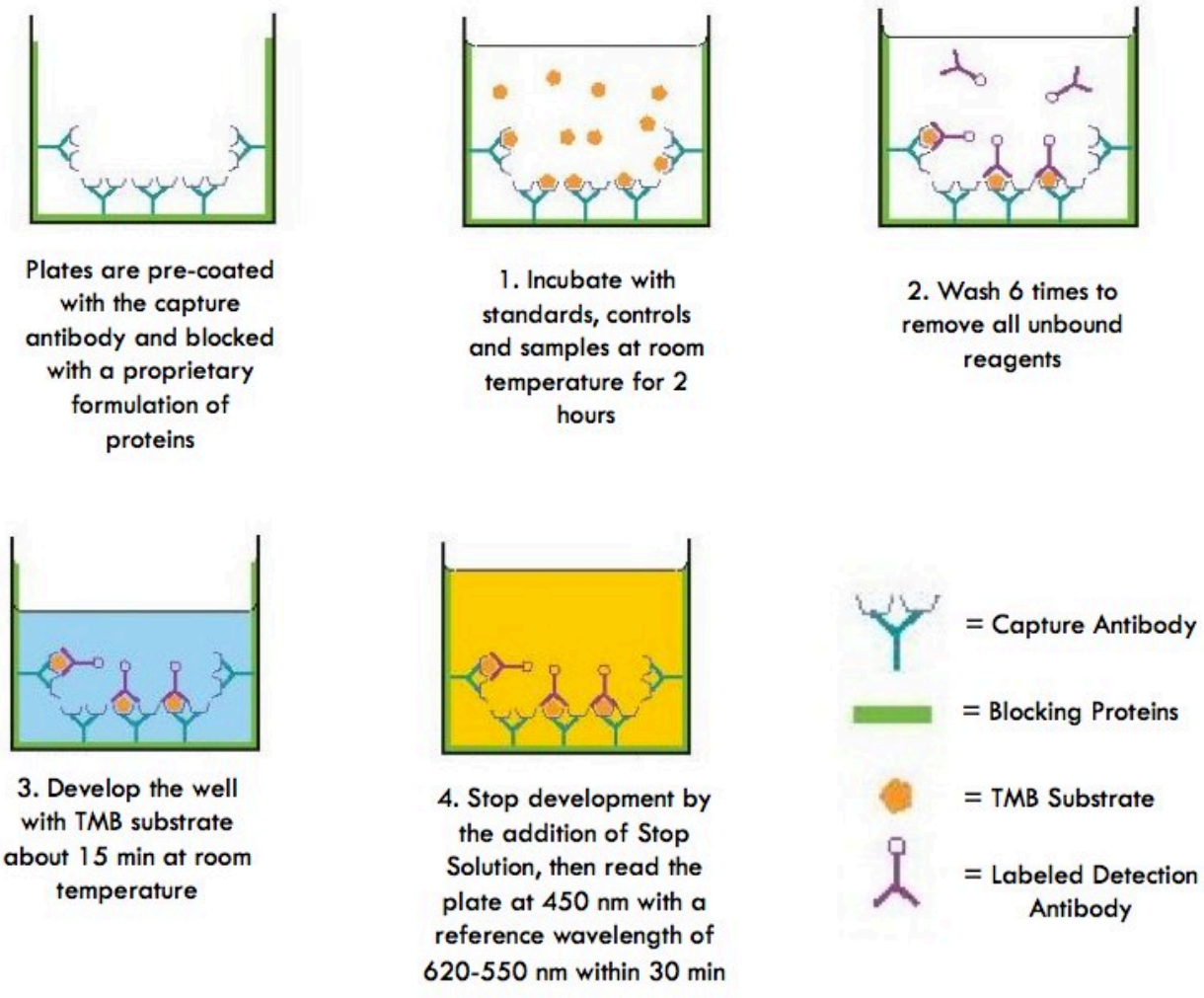

Figure 3. 9. ELISA Immunoassay Analysis Principle

	1	2	3	4	5	6	7	8	9	10	11	12
A	BL	BL	1	17	33	49	9	25	41	57	65	81
B	S1	S1	2	18	34	50	10	26	42	58	66	82
C	S2	S2	3	19	35	51	11	27	43	59	67	83
D	S3	S3	4	20	36	52	12	28	44	60	68	84
E	S4	S4	5	21	37	53	13	29	45	61	69	85
F	S5	S5	6	22	38	54	14	30	46	62	70	86
G	QC1	QC1	7	23	39	55	15	31	47	63	71	87
H	QC2	QC2	8	24	40	56	16	32	48	64	72	88

Figure 3. 10. ELISA Analysis Plate Design with End Color Development. Arrangement of the samples on a 96-well plate 01–88: samples (sample dilution L: 1:10; H: 1:20); BL, L1–L5: standards, QC1 and QC2 quality controls).

3.3 Statistics

The cell viability assay (MTT) experiments were performed two times with a sample size of n = 4 per replicate. The SEM, LSCM experiments were performed two times with a sample size of n= 2 per replicate, while the ELISA analysis was performed only once with a sample size of n = 2. All values were reported in terms of the mean ± standard deviation. A comparison between the test group and the controls was performed by an ANOVA test. A p-value of $\leq$ 0.05 was considered statistically significant.

Chapter 4 Results and Discussion

4.1 Scaffold Structure Evaluation

The first part of the study was to evaluate the structure of the scaffolds. We included two kinds of warp knitted scaffolds in our study; a 12 gauge and 24 gauge spacer fabric. The major difference between them was the average pore size and total porosity of the structures, which resulted in quite different biological performances for the specific cell line of islet cells. The objective of this experiment was to find the preferred structure that would support Beta-TC-6 islet cells viability and proliferation.

4.1.1 Scanning Electron Microscope (SEM)

A scanning electron microscope was utilized to visualize and confirm the level of cell attachment on the surface of the scaffolds after 7 days of culture. As shown in Figures 4.1 and 4.2, it was clear that the cells had attached and were proliferating on both the 12 gauge and 24 gauge scaffold surfaces. However, by Day 7 there appeared to be more cells and larger clusters of cells on the 24 gauge scaffold than 12 gauge sample.

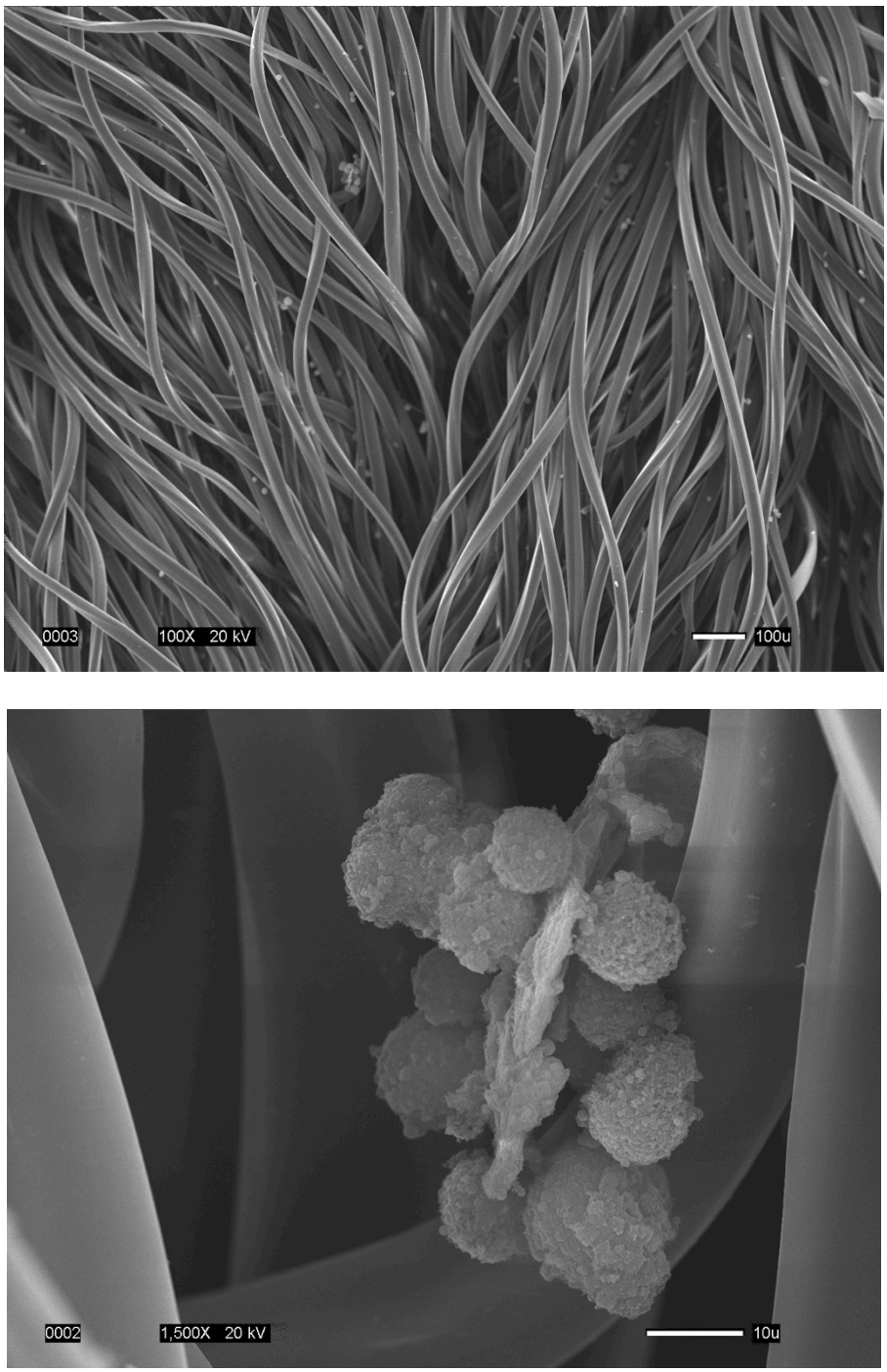

Figure 4. 1. SEM Images of 12 Gauge Polyester 3D Scaffold after 7 Days of Culture.

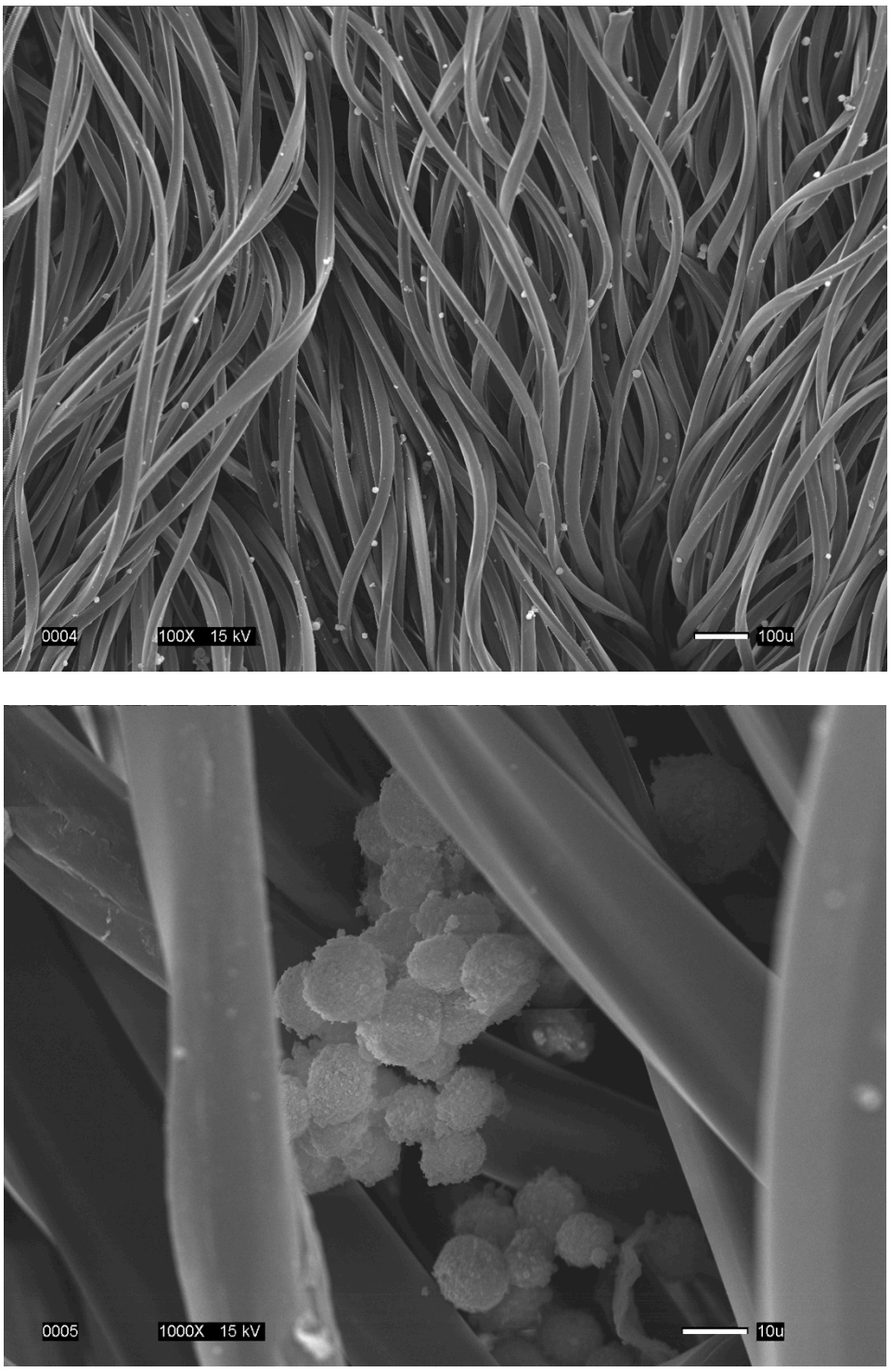

Figure 4. 2. SEM Images of 24 Gauge Polyester 3D Scaffold after 7 Days of Culture.

4.1.2 Laser Scanning Confocal Microscope (LSCM)

Since SEM was limited to only viewing the surface of the scaffolds, laser scanning confocal microscopy (LSCM) with DAPI staining of the nuclei (shown in green in the LSCM images) was used to observe the amount of cell attachment and migration through the thickness of the scaffolds (Figures 4.3 and 4.4). It was evident that the islet cells had migrated through the thickness of scaffolds in 5 days of culture, and were continuing their migration on both the 12 gauge and 24 gauge fiber scaffolds during the 10-day culture period. However, it was difficult to quantify the total cell number on the two types of scaffolds and determine whether there were differences.

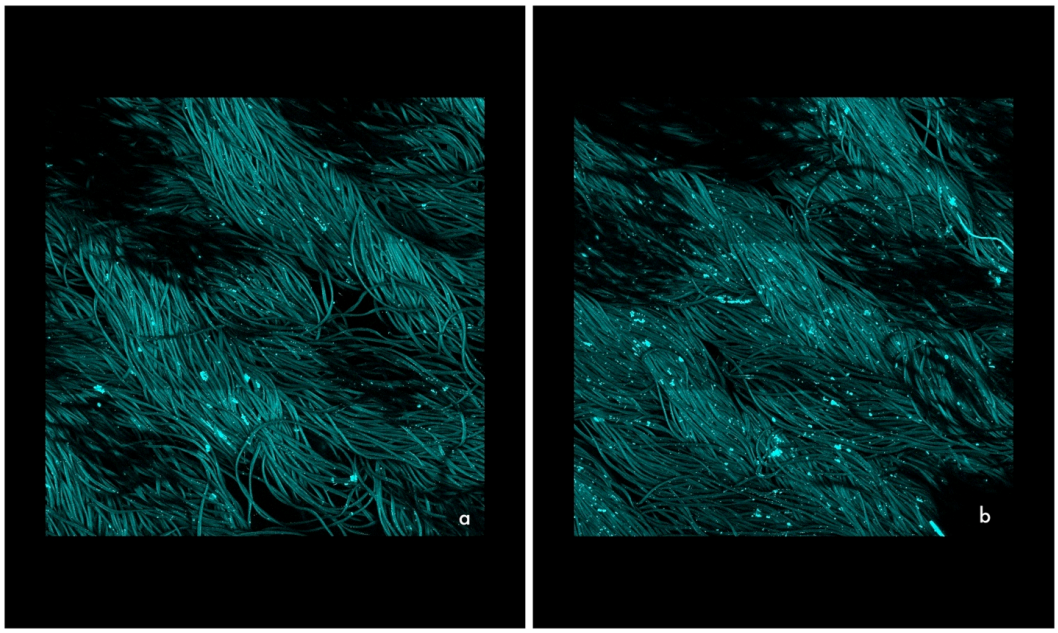

Figure 4. 3. LSCM Images of Polyester 3D Scaffold after 5 Days of Culture. (a) 12 Gauge Scaffold; (b) 24 Gauge Scaffold.

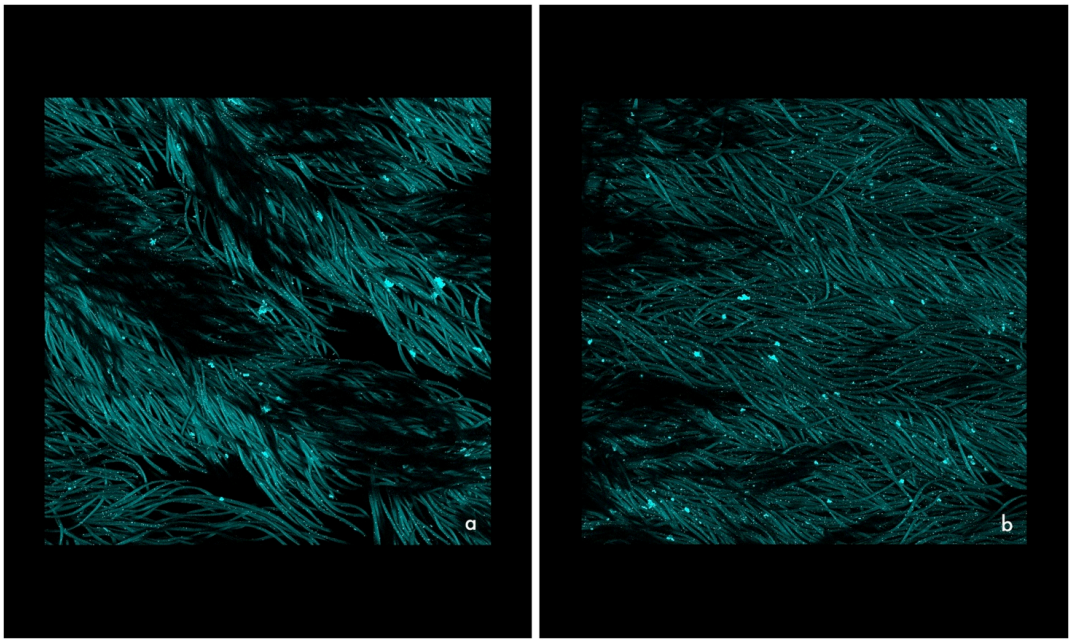

Figure 4. 4. LSCM Images of Polyester 3D Scaffold after 10 Days of Culture. (a) 12 Gauge Scaffold; (b) 24 Gauge Scaffold.

4.2 Surface Modification Evaluation

The MTT cell viability assay was used to evaluate the effect of surface modification on cell growth. The PLA nonwoven 2 dimensional (2D) scaffold without coating (S1) was compared with three different surfaces: collagen coated without activation (S2); maleic acid activated, genipin treated and immobilized collagen (S3) and maleic acid activated and genipin treated, but without immobilized collagen (S4) (See Table 4.1). A 3 day and 7 day static cell culture experiment was performed with beta-TC-6 islet cells. Cells were seeded in duplicate onto the four different kinds of treated and untreated PLA scaffolds as described above with a seeding

density of 7,500 cells/well using 24-well plates. At each time point, the scaffolds were transferred to new plates for the MTT assay.

Table 4. 1. Description of Four Samples of PLA Nonwoven Scaffolds.

Sample ID	**Sample Description**
S1 (PLA control)	PLA untreated
S2 (collagen)	PLA without surface activation, coated with collagen
S3 (maleic acid + genipin + collagen)	PLA grafted with maleic acid, and genipin and then immobilized with collagen
S4 (maleic acid + genipin)	PLA grafted with maleic acid and genipin only

4.2.1 MTT Cell Viability Assay

The MTT viability assay was performed in order to obtain a direct count of viable beta-TC-6 islet cells. Regression analysis of the results indicates that there was a direct and positive correlation between the number of cells counted and the MTT absorbency reading at 540 nm. The linear relationship between the cell number and the optical density (OD) values can be expressed by the formula: $y = 0.4998x - 0.4722$ ($R^2 = 0.99862$) as shown in Figure 4.5. The viable cell numbers attached to the 3D PET 24 gauge scaffolds at different time points was determined from this calibration curve.

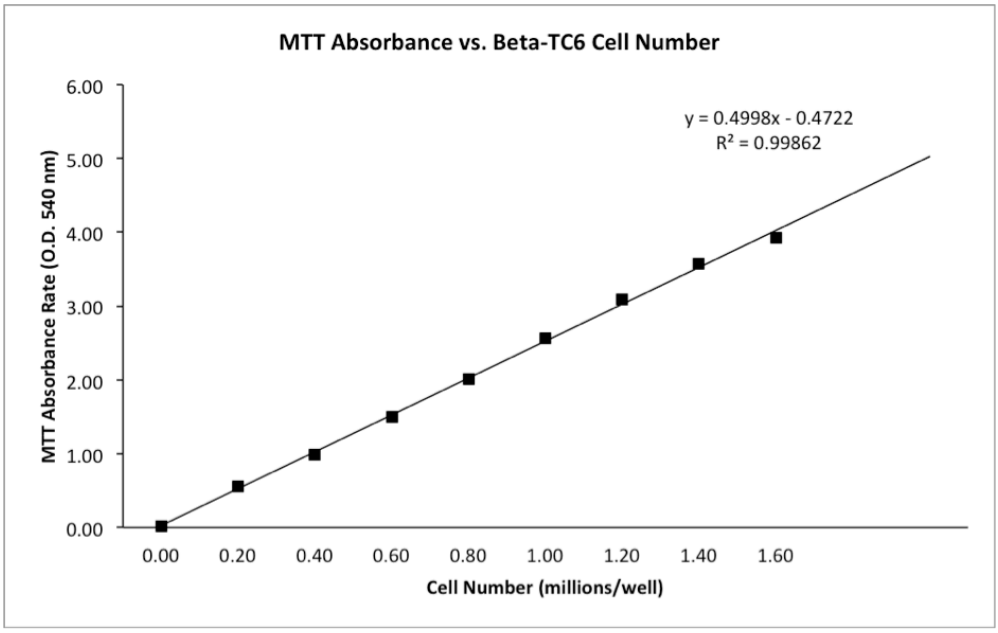

Figure 4. 5. Cell Number Calibration Curve for MTT Assay.

For the purpose of evaluating cell attachment and proliferation, another MTT assay using static culture conditions was conducted at 3 and 7 days as shown in Figure 4.6. The MTT results were acquired as optical density values in the form of absorbance readings at 540 nm. A higher absorbance value indicates higher amount of cell viability. For each well after the reaction, the supernatant was carefully transferred (100 μ-L/ time) to 3 new 96-well plates for spectrophotometric analysis. The MTT assay results are reported as relative absorbance as shown in Table 4.2 and Figure 4.6 with the mean value and the standard deviation of the mean represented by an error bar (sample size = 4). The relative values were obtained by subtracting the mean absorbance of the blank wells, which was 0.025 with a standard deviation of 0.001.

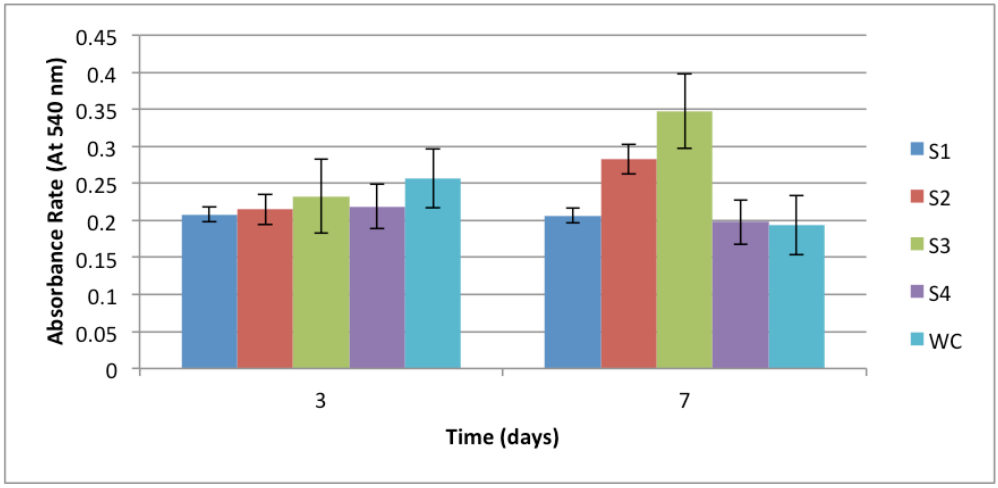

Figure 4. 6. MTT Assay of PLA Nonwoven Scaffolds Seeded with Beta-TC6 Murine Pancreatic Cells. Error bars = standard deviation. WC = well control.

Table 4. 2. Optical Density (OD) Values for Each Sample. (mean ± standard deviation)

	3 Days	*7 Days*
S1	0.208±0.012	0.206 ± 0.033
S2	0.214 ±0.023	0.283 ± 0.050
S3	0.233±0.020	0.347 ± 0.023
S4	0.219±0.013	0.198 ± 0.045
WC	0.257±0.020	0.193 ± 0.031

The above results indicate that S3, the sample with collagen immobilized on a maleic acid activated and genipin treated surface had the highest average OD values. This means that it had the largest number of viable cells after both 3 days and 7 days in culture. Sample S1, the

untreated sample, the sample without collagen S4 and the well controls (WC) showed similar behavior. Among them the well controls showed the least cell viability among all the samples. Sample S2, the collagen coated scaffold, but without any surface activation to immobilize the collagen onto the scaffold, showed some cell proliferation, but less than Sample S3, which had collagen immobilized on the activated and genipin treated surface.

4.3 Evaluation of Collagen Coated 3D Scaffold (24 Gauge)

In this section of the study, we extended the work described in the previous two sections by examining the performance of one particular scaffold structure with the objective of determining which surface modification method would best support beta-TC-6 cells viability and proliferation. Consequently we evaluated the ability of the 24 gauge 3D PET scaffold coated with Type I collagen to promote beta-TC-6 cell viability, proliferation and insulin secretion at 0, 3, 7 and 10 day time points. This experiment would provide insight into how the scaffold coated with ECM protein might enhance both the survival and function of beta-TC-6 cells.

4.3.1 Time-of-Flight Secondary Ion Mass Spectrometry (TOF-SIMS)

The TOF-SIMS technique is a surface sensitive approach to providing semi-quantitative data about surface chemistry. It was used to monitor the presence and uniformity of the collagen coating on the 3D PET 24 gauge scaffold top (face) surface and cross-sectional surface after

collagen coating. The collagen coated scaffold samples were compared with untreated scaffold samples. The results of chemical mapping conducted using the TOF-SIMS signals are shown in Figures 4.7 and 4.8.

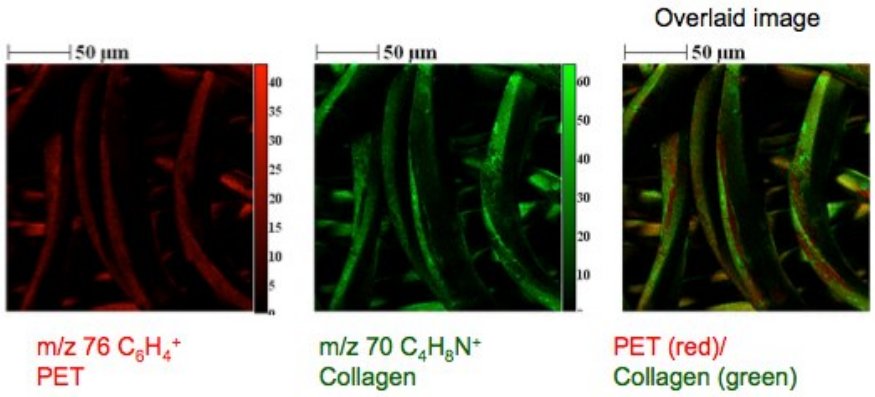

Figure 4. 7. Positive Ion Images of Coated Surface (200 um X 200 um)

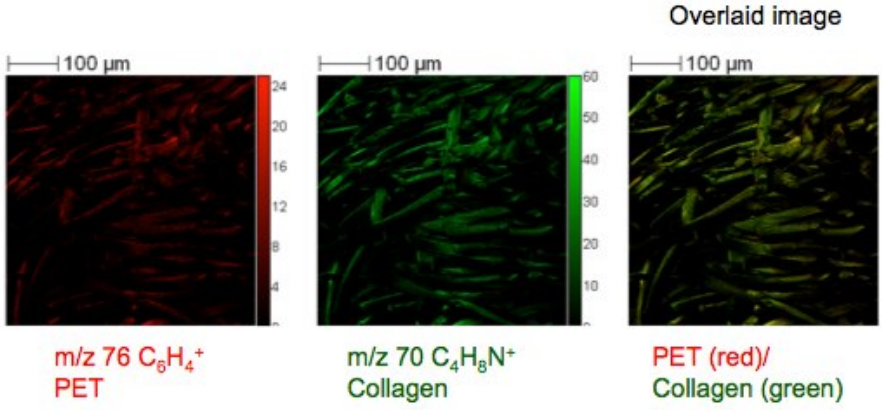

Figure 4. 8. Positive Ion Images of Cross Section (500 um X 500 um)

Figure 4.7 shows the images obtained from the top (face) surface of the scaffolds. It can be seen that the collagen was coated and distributed uniformly on the face of the scaffold.

Figure 4.8 shows the images obtained from the cross-sectional views of the 3D scaffold. They confirm that the collagen was able to penetrate through the thickness of the scaffold. Both Figures 4.7 and 4.8 show good continuous collagen coverage with only a few red spots, which identify exposed PET substrate. This suggests that the 3D scaffolds were successfully coated with Type I collagen and achieved a satisfactory uniform collagen distribution.

4.3.2 Contact Angle

The contact angle images were obtained using an OCA 20 Model DataPhysics video-based optical contact angle system with SCA 20 software. The treated and untreated scaffolds were compared under the same test conditions as shown in Figures 4.9, 4.10 and 4.11. This was repeated at five different locations across each sample so as to obtain representative data from the whole sample.

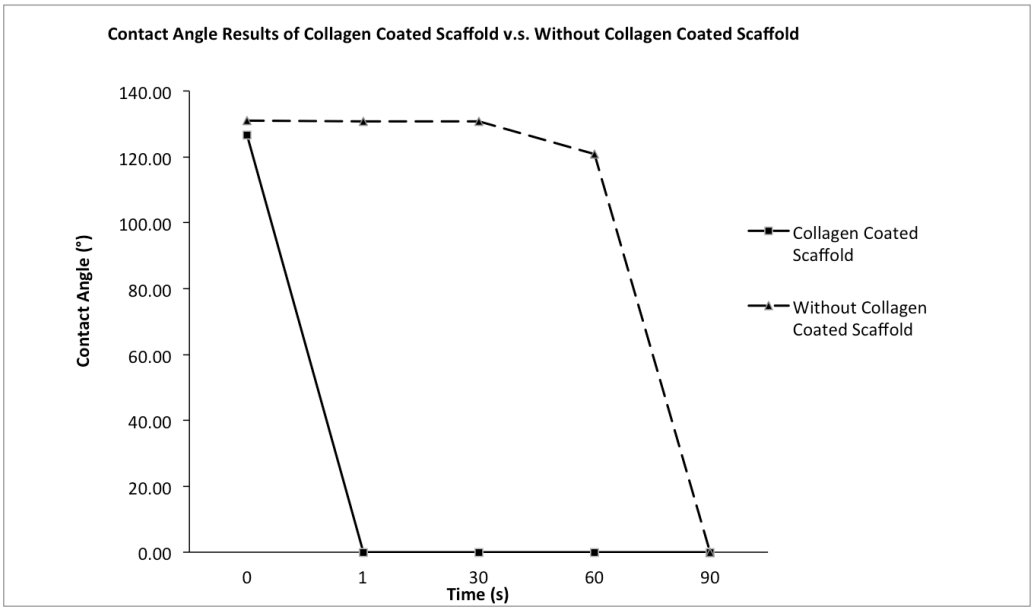

Figure 4. 9. Contact Angle Results of Collagen Coated 24 gauge PET Scaffold v.s. Without Collagen Coated 24 gauge PET Scaffold.

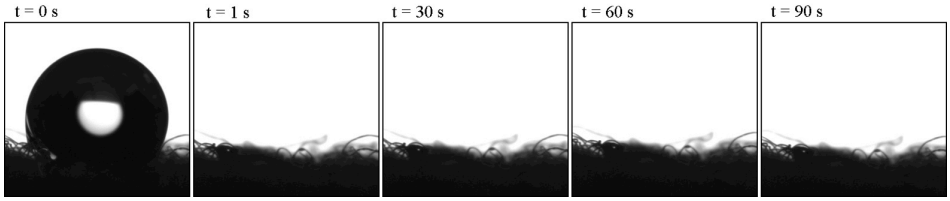

Figure 4. 10. Contact Angle Results for Collagen Coated PET Scaffold.

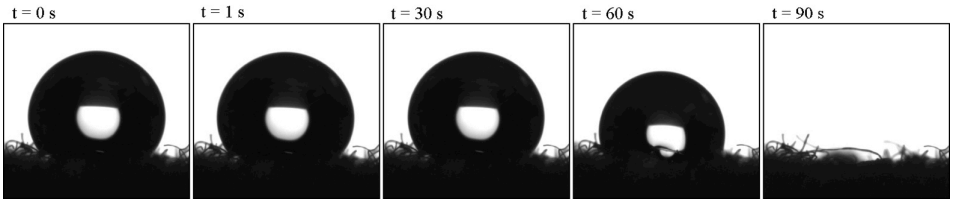

Figure 4. 11. Contact Angle Results for PET Scaffold Without Collagen Coating.

Figure 4.10 shows that after Type I collagen coating, the droplet instantly disappeared within the first second compared to the PET scaffold without collagen coating. In this case, the droplet disappeared after at least 60 s due to the lower hydrophilicity and the slower moisture transport of the scaffold surface (see Figure 4.11).

4.3.3 Cell Viability Assay (MTT)

For the purpose of evaluating cell attachment and proliferation, MTT assay using static culture conditions was conducted at 0, 3, 7, and 10 days as shown in Figure 4.12. The original data set is presented in Table 4.3. In addition to the test group, beta-TC-6 cells were also cultured on a scaffold without collagen and without any scaffold material, which served as controls. Throughout the 10-day culture period, increasing numbers of cells attached and proliferated on the collagen-coated scaffold, showing significant differences during the culture period ($p < 0.05$).

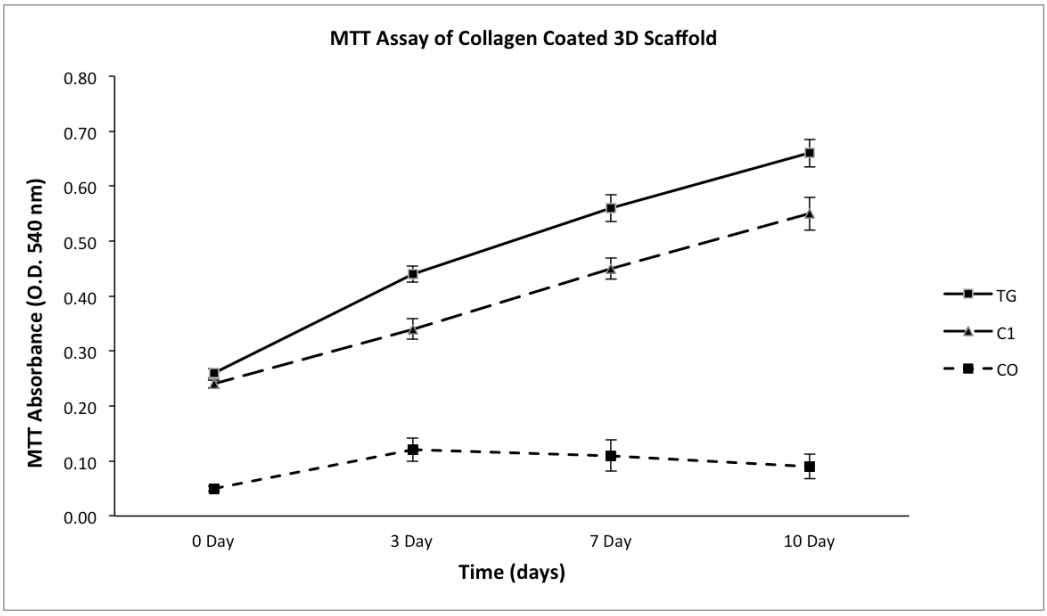

Figure 4. 12. Results of MTT Assay for Cell Viability. TG: Test Group (Collagen Coated Scaffold)C1: Control Group Scaffold Without Collagen; CO: Cell Only.

Table 4. 3. Results of MTT Assay for Cell Viability Means and Standard Deviations of Absorbance at O.D. = 540 nm. TG: Test Group (Collagen Coated Scaffold); C1: Control Group Scaffold Without Collagen; CO: Cell Only.

	TG		**C1**		**CO**	
	Mean	S.D.	Mean	S.D.	Mean	S.D.
0 Day	0.256	0.009	0.243	0.007	0.05	0.005
3 Day	0.442	0.015	0.344	0.019	0.12	0.021
7 Day	0.563	0.025	0.453	0.019	0.11	0.029
10 Day	0.656	0.025	0.550	0.03	0.09	0.022

4.3.4 Cell Morphology on Scaffold Surface (SEM)

The scanning electron microscope was utilized to visually confirm the level of cell adhesion and proliferation on the surfaces of the both collagen coated scaffolds and the scaffolds without collagen. Figure 4.13 shows the fibrous structure of the scaffolds before cell seeding. From the SEM images it is evident that the collagen coating process improved the smoothness of the fibers compare to the fibers without collagen. This meant that the collagen coating process may have created more cell adhesion points. This was confirmed by viewing the 3 day (Figure 4.14), 7 day (Figure 4.15) and 10 day (Figure 4.16) SEM images. These results are in agreement with the findings of the MTT cell proliferation assay, LSCM cell migration observations and insulin production analysis. These images provide two consistent observations. First, more cells were visualized on the collagen coated scaffold surface. Second, better cell adhesion and proliferation with larger aggregates of cells were observed on the collagen coated scaffold surface, which agrees with later MTT results.

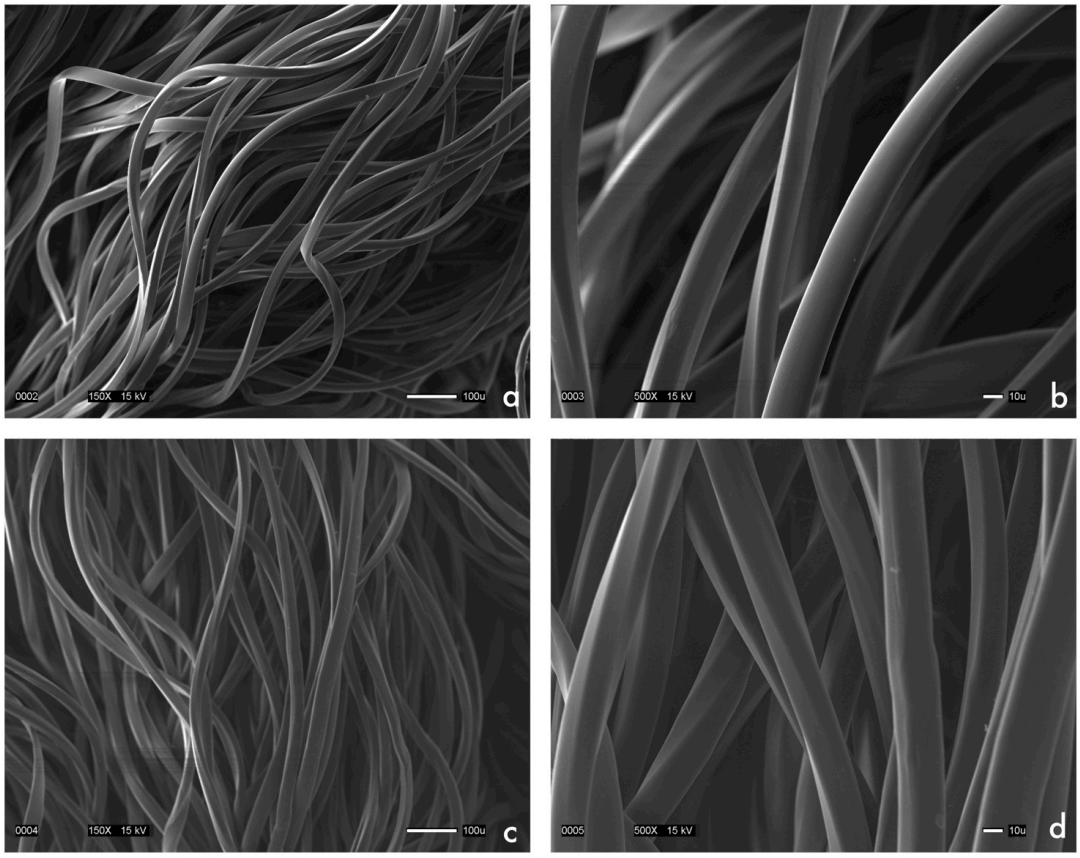

Figure 4.13. 24 Gauge 3D PET Scaffolds before Cell Seeding. (a). 150x scaffold without collagen coating; (b) 1,000x scaffold without collagen coating; (c). 150x collagen coated scaffold; (d) 1,000x collagen coated scaffold.

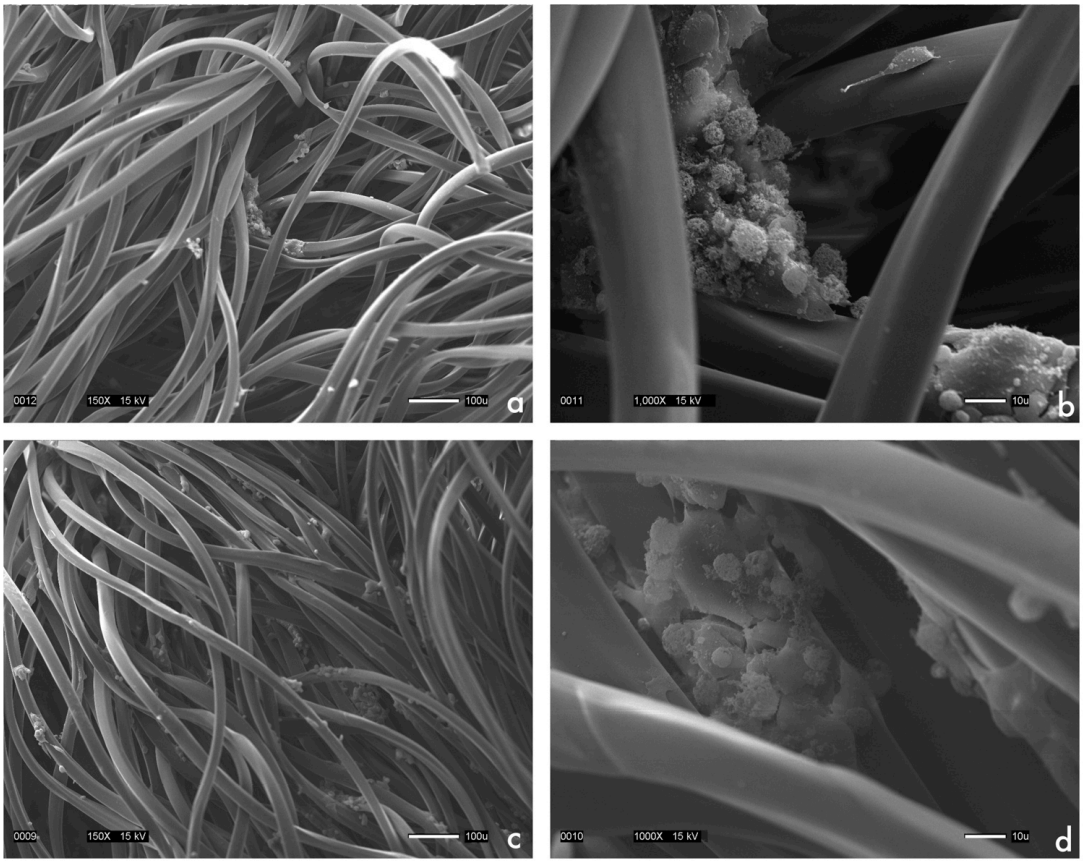

Figure 4.14. Day 3 Results of 24 Gauge 3D PET Scaffold after Cell Seeding. (a). 150x scaffold without collagen coating; (b) 1,000x scaffold without collagen coating; (c). 150x collagen coated scaffold; (d) 1,000x collagen coated scaffold.

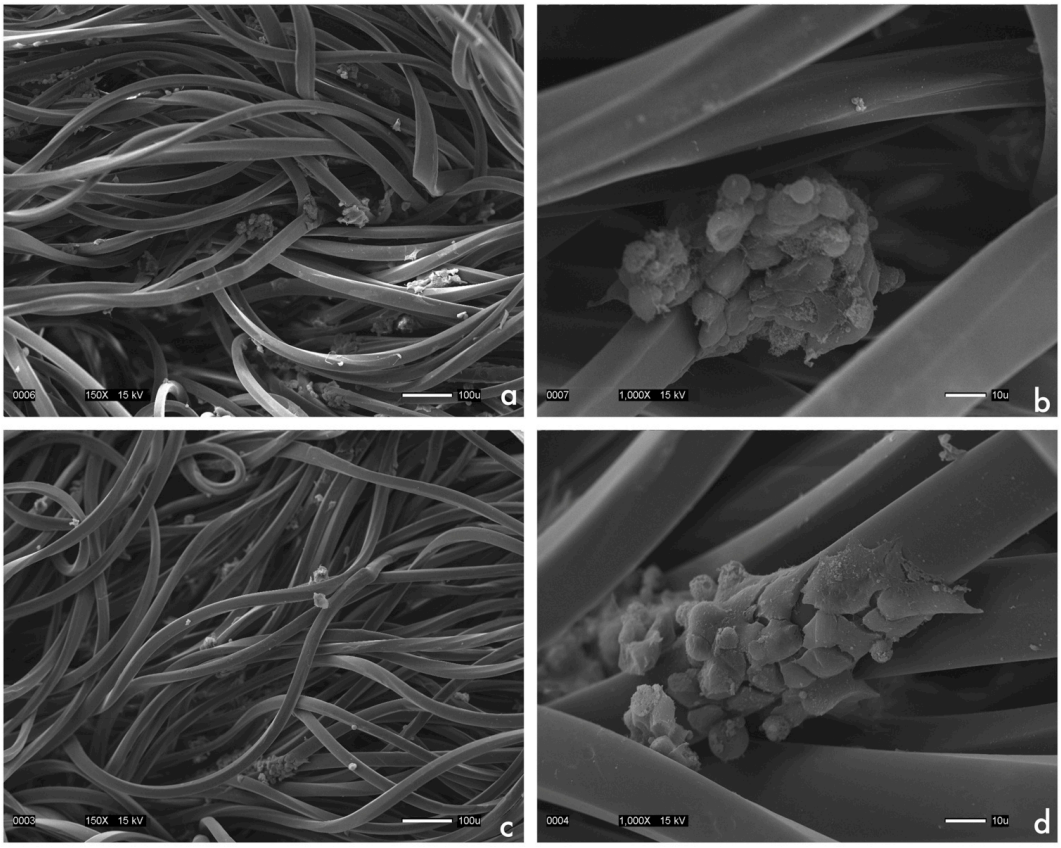

Figure 4.15. Day 7 Results of 24 Gauge 3D PET Scaffold after Cell Seeding. (a). 150x scaffold without collagen coating; (b) 1,000x scaffold without collagen coating; (c). 150x collagen coated scaffold; (d) 1,000x collagen coated scaffold.

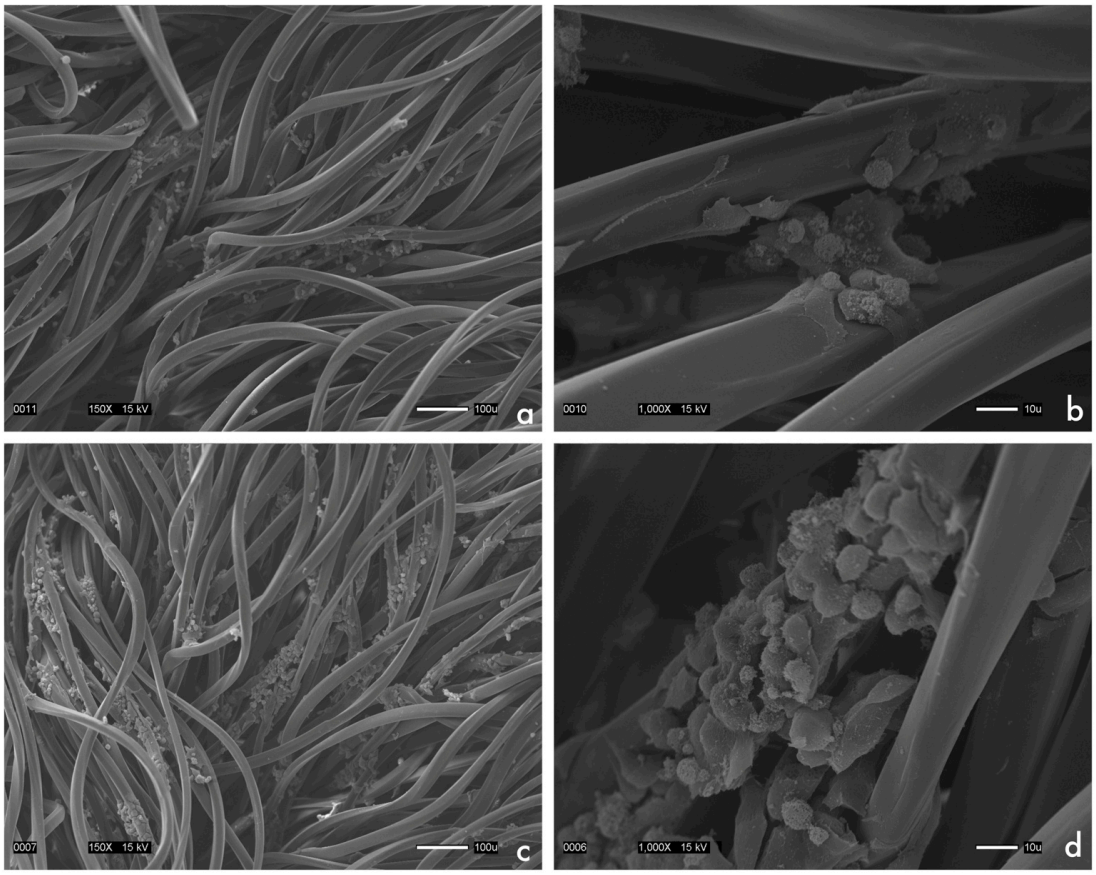

Figure 4.16. Day 10 Results of 24 Gauge 3D PET Scaffold after Cell Seeding. (a). 150x scaffold without collagen coating; (b) 1,000x scaffold without collagen coating; (c). 150x collagen coated scaffold; (d) 1,000x collagen coated scaffold.

4.3.5 Cell Migration throughout the 3D Scaffold (LSCM)

The PI stain is capable of staining the nuclei of dead cells red under the laser scanning confocal microscope. LSCM is a technique that is used to observe cell migration inside the scaffold structure so as to provide information about cell migration and proliferation

throughout the thickness of the scaffold. This approach differs from SEM which is used to observe cell morphology and attachment on the outside of the scaffold surface. The LSCM images were obtained at 3, 7 and 10 days of cell culture, and are presented in Figures 4.17, 4.18 and 4.19 respectively.

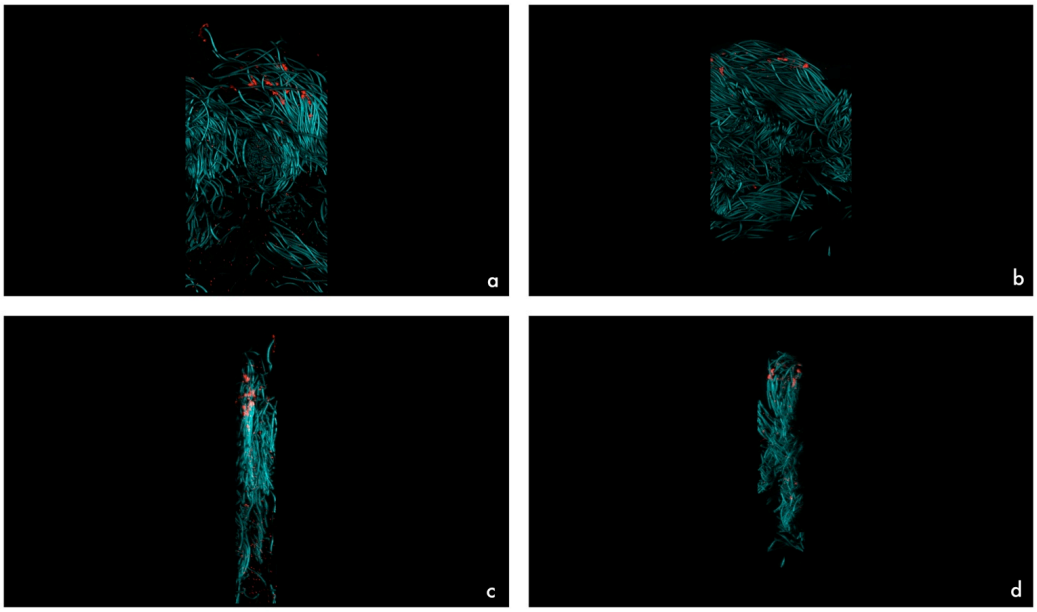

Figure 4. 17. Day 3 LSCM Results. (a) Cross-section of collagen coated scaffold; (b) Cross-section of scaffold without collagen coating; (c) 90° view of cross-section of collagen coated scaffold; (d) 90° view of cross-section of scaffold without collagen coating.

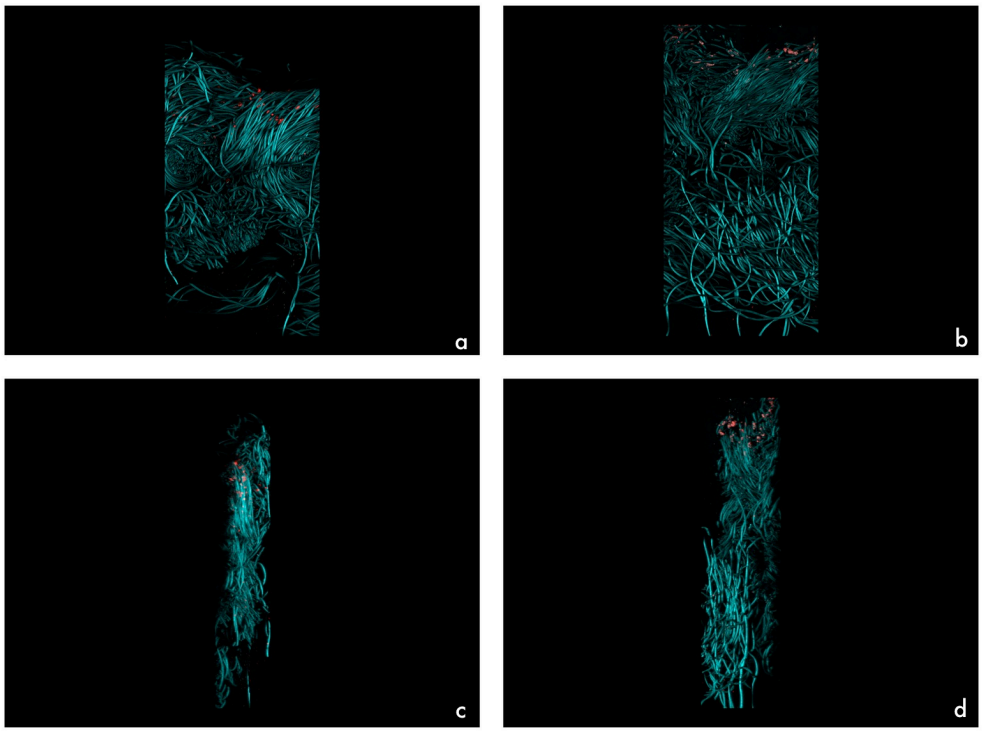

Figure 4. 18. Day 7 LSCM Results. (a) Cross-section of collagen coated scaffold; (b) Cross-section of scaffold without collagen coating; (c) 90° view of cross-section of collagen coated scaffold; (d) 90° view of cross-section of scaffold without collagen coating.

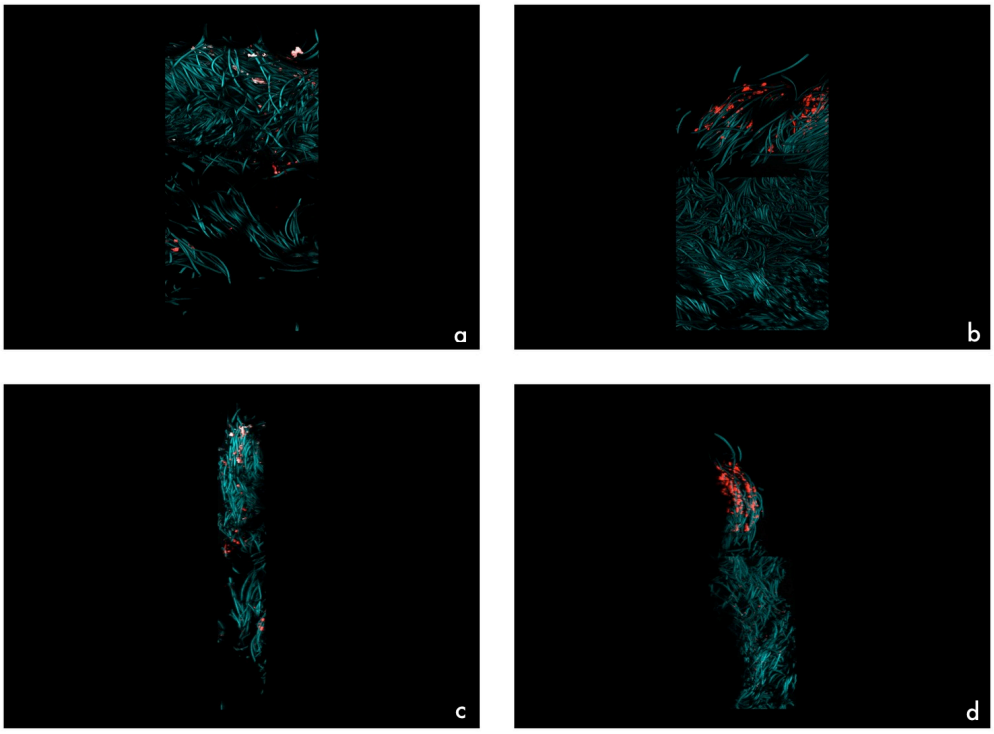

Figure 4. 19. Day 10 LSCM Results. (a) Cross-section of collagen coated scaffold; (b) Cross-section of scaffold without collagen coating; (c) 90° view of cross-section of collagen coated scaffold; (d) 90° view of cross-section of scaffold without collagen coating.

Figure 4.17 shows that by Day 3 the cells were starting to migrate along the collagen coated fibers of the coated scaffold, whereas the untreated scaffold appeared to have few observable cells. Figure 4.18 shows the LSCM images after 7 days of culture. In this figure we observe that the cells have migrated half-way through the thickness of the collagen coated scaffold whereas the cells on the untreated fibers appeared to aggregate close to the top surface of the scaffold. After 10 days of cell culture the LSCM images showed that the cells on the collagen

coated fibers had migrated throughout the thickness of the scaffold, in contrast, to the untreated scaffold images, which showed that the cells had migrated only about one quarter the depth of the whole scaffold thickness (Figure 4.19).

4.3.6 Detection of Islet Cell Function (ELISA Immunoassay)

Using an ELISA immunoassay the functionality of the beta-TC-6 islet cells was analyzed in terms of insulin production under high and low glucose conditions. Insulin generation was measured after 0, 3, 7 and 10 days of cell culture on both types of scaffolds with and without collagen coating. Empty wells containing no scaffold and without any scaffold material were also included as a control group. Figures 4.20, 4.21, 4.22 and 4.23 illustrate the original data that is presented in Tables 4.4, 4.5, 4.6, and 4.7 respectively. The overall trend shows that insulin production increased during the first hour, but then began to decrease between 2 and 4 hours. At each time point, the beta-TC-6 islet cells cultured on 3D scaffolds indicated an enhanced production compared with cells cultured in the control 2D plate wells ($p < 0.05$). This was especially true for those cells cultured on collagen coated scaffolds which exhibited the highest insulin release index among all three groups. From this we conclude that a 3D scaffold, and especially a 3D scaffold with an ECM collagen protein coating, is an essential scaffold requirement in order to support the proliferation and functionality of beta-TC-6 islet cells to express insulin *in vitro*.

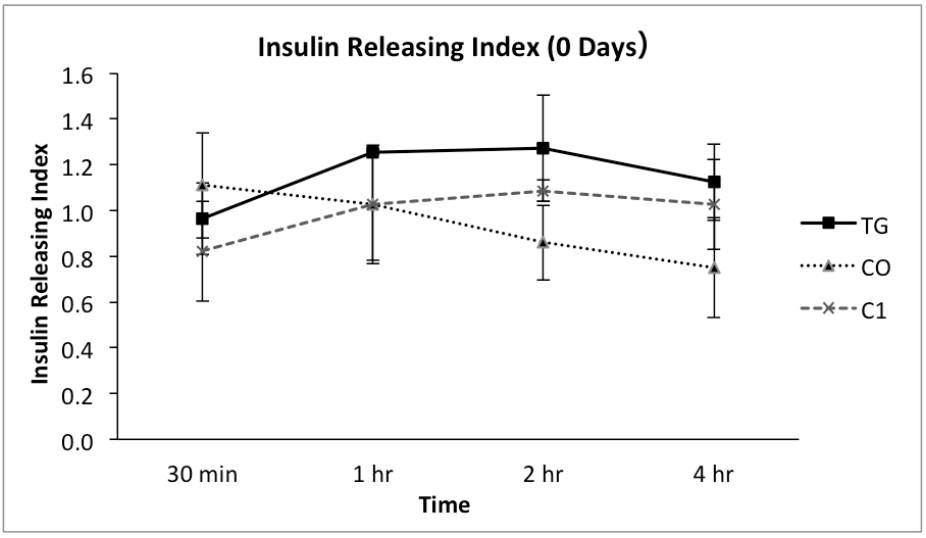

Figure 4. 20. Day 0 Results of Insulin Releasing Index.

TG: Test Group (Collagen Coated Scaffold) CO: Cells Only; C1: Control Group Scaffold Without Collagen. Error bar = standard deviation

Table 4. 4. Day 0 Results of Insulin Releasing Index. Means and Standard Deviations: TG: Test Group (Collagen Coated Scaffold) CO: Cells Only; C1: Control Group Scaffold Without Collagen

0 Day	**30 min**	**1 hr**	**2 hr**	**4 hr**
TG Mean	0.963	1.256	1.273	1.125
TG S.D.	0.156	0.010	0.232	0.168
CO Mean	1.111	1.026	0.860	0.750
CO S.D.	0.231	0.243	0.164	0.218
C1 Mean	0.823	1.026	1.087	1.025
C1 S.D.	0.219	0.259	0.048	0.197

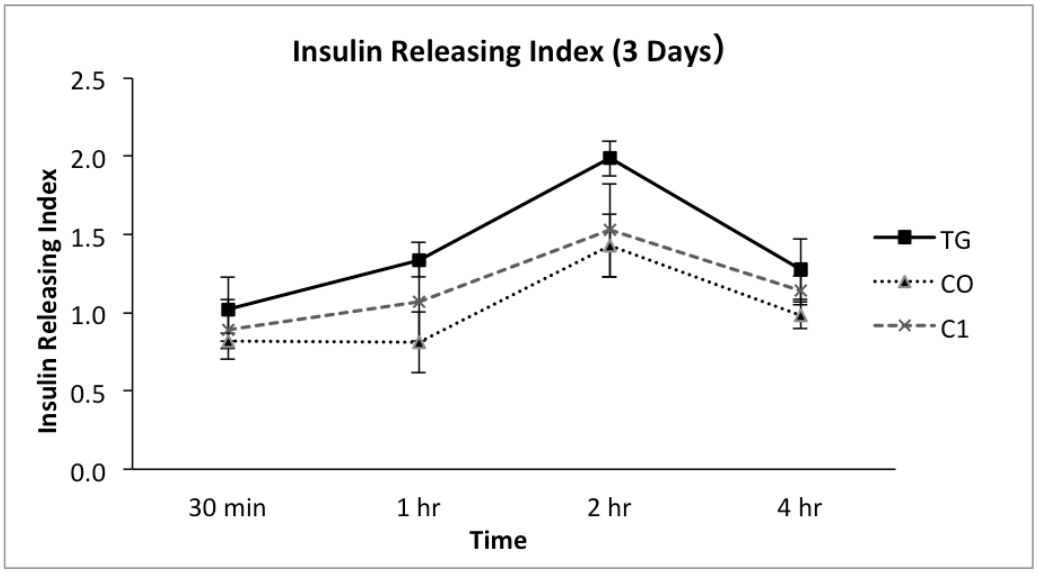

Figure 4. 21. Day 3 Results of Insulin Releasing Index.

TG: Test Group (Collagen Coated Scaffold) CO: Cells Only; C1: Control Group Scaffold Without Collagen. Error bar = standard deviation

Table 4. 5. Day 3 Results of Insulin Releasing Index. Means and Standard Deviations: TG: Test Group (Collagen Coated Scaffold); CO: Cells Only; C1: Control Group Scaffold Without Collagen

3 Day	30 min	1 hr	2 hr	4 hr
TG Mean	1.023	1.339	1.986	1.280
TG S.D.	0.206	0.109	0.112	0.194
CO Mean	0.822	0.811	1.430	0.983
CO S.D.	0.051	0.195	0.199	0.084
C1 Mean	0.891	1.071	1.527	1.144
C1 S.D.	0.190	0.251	0.298	0.093

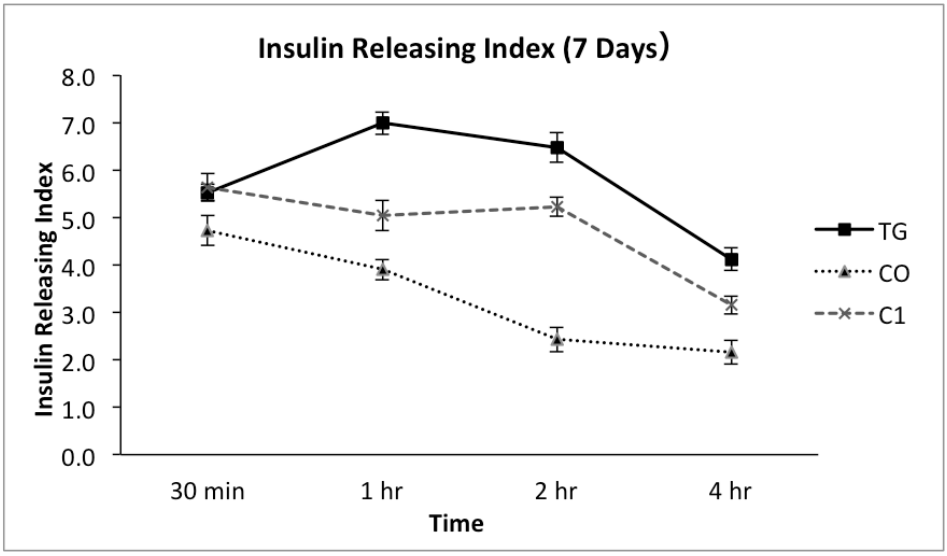

Figure 4. 22. Day 7 Results of Insulin Releasing Index.

TG: Test Group (Collagen Coated Scaffold); CO: Cells Only; C1: Control Group Scaffold Without Collagen. Error bar = standard deviation

Table 4. 6. Day 7 Results of Insulin Releasing Index. Means and Standard Deviations: TG: Test Group (Collagen Coated Scaffold) CO: Cells Only; C1: Control Group Scaffold Without Collagen.

7 Day	30 min	1 hr	2 hr	4 hr
TG Mean	5.523	6.988	6.480	4.118
TG S.D.	0.178	0.236	0.317	0.243
CO Mean	4.729	3.897	2.425	2.154
CO S.D.	0.316	0.211	0.255	0.253
C1 Mean	5.635	5.041	5.225	3.154
C1 S.D.	0.283	0.319	0.199	0.188

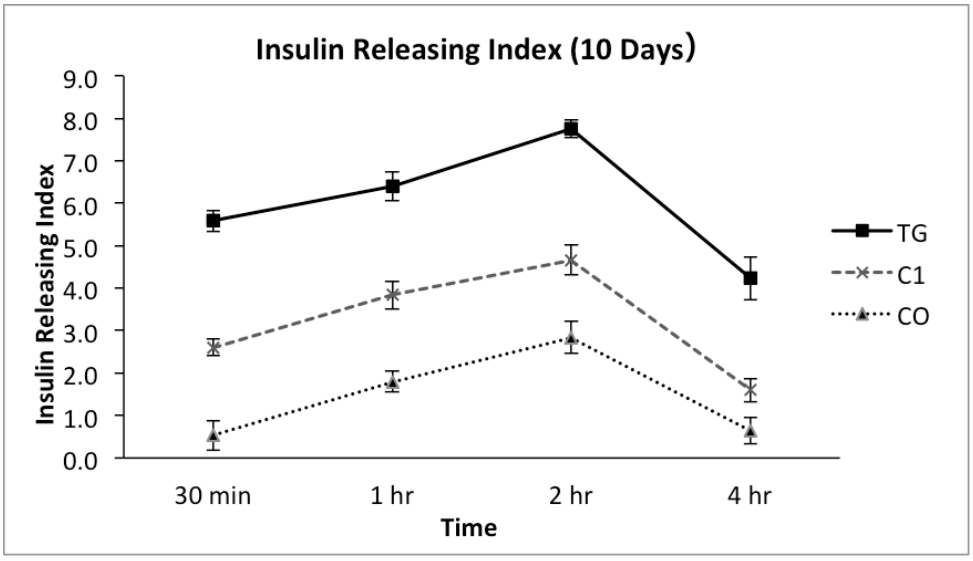

Figure 4. 23. Day 10 Results of Insulin Releasing Index.

TG: Test Group (Collagen Coated Scaffold) CO: Cells Only; C1: Control Group Scaffold Collagen Coated. Error bar = standard deviation

Table 4. 7. Day 10 Results of Insulin Releasing Index. Means and Standard Deviations: TG: Test Group (Collagen Coated Scaffold); CO: Cells Only; C1: Control Group Scaffold Without Collagen

10 Day	30 min	1 hr	2 hr	4 hr
TG Mean	5.585	6.402	7.752	4.227
TG S.D.	0.248	0.345	0.203	0.498
CO Mean	0.534	1.800	2.838	0.641
CO S.D.	0.350	0.242	0.371	0.306
C1 Mean	2.606	3.836	4.661	1.601
C1 S.D.	0.204	0.327	0.357	0.278

Chapter 5 Conclusions and Recommendations

5.1 Conclusions

In Chapter 1 the goals and three specific objectives of this study are described. Here in the conclusion section, we return to those objectives and comment on whether each one was achieved, and if so what were the specific findings for each conclusion.

1) The 24 gauge 3D PET warp knitted spacer fabric scaffold with the smaller pore size was more effective in supporting beta-TC-6 islet cell proliferation and migration through the thickness of the 3 mm thick scaffold.
2) The 2D nonwoven PLA scaffold activated with maleic acid, treated with genipin and immobilized with Type I collagen offers superior beta-TC-6 islet cell viability according to the MTT assay.
3) The results from the beta-TC6 islet *in vitro* cell culture experiment on a Type I collagen coated 3 mm thick 24 gauge 3D PET spacer fabric scaffold showed that the presence of collagen is advantageous for beta-TC-6 islet cell growth, migration, and functionality in terms of insulin production. In conclusion, it is believed that the smaller average pore size and better cell-collagen interface supports the growth, proliferation and function of islet-like aggregates *in vitro*.

5.2 Further Work

In the future it is recommended that more detailed beta-TC-6 islet cell proliferation and function experiments be undertaken to help in gathering useful information on different types of scaffolds in terms of polymer type, rate of resorption, geometric structure and surface modification. The experiments should be performed in triplicate in order to confirm the results with statistical confidence.

Another additional step in this research study would involve the fabrication of a surface modified 3D 24 gauge scaffold knitted from PLA yarns and activated with maleic acid, treated with genipin and immobilized with Type I collagen. This scaffold will be biodegradable, and the degradation time needs to be investigated to better integrate the time to maturity for the islet cells with the rate of resorption of the scaffold after implantation.

An additional study would involve the generation of a surface modified 3D PLA scaffold containing a prevascularized tissue engineered network of endothelial cells before seeding islet cells. This prevascularized construct would likely play an essential role in islet transplantation, because it would provide easy access for islet seeding, promote islet viability, proliferation and function, and could be easily retrieved and transplanted to alternative anatomical sites by microvascular methods [135].

In addition, the use of the surface modified 3D biodegradable knitted spacer fabric scaffolds fabricated by our group will serve as an interesting candidate for further studies in a range of different tissue engineering applications including vascular, urological, orthopedic and dental end-uses. They could be used as basic tissue engineering research tools, and ultimately find applications in clinical therapy.

REFERENCES

1. Darcy B., W. (2005). Immunology insulin auto-antigenicity in type 1 diabetes. *Nature*, 438, E5.
2. Yang, Y. (2006). Biodegradable scaffolds - delivery systems for cell therapies. *Expert Opinion on Biological Therapy*, 6(5), 485-498.
3. Williams, D. F. (2003). Biomaterials and tissue engineering in reconstructive surgery. *Sadhana*, 28(3), 563-574.
4. Niklason, L. E. (2001). Prospects for organ and tissue replacement. *JAMA*, 285(5), 573-576.
5. Langer R, & Vacanti JP. (1993) Tissue engineering. *Science,* 260 (5110):920-8.
6. Chapekar, M. S. (2000). Tissue engineering: Challenges and opportunities. *J Biomed Mater Res*, 53, 617-620.
7. Dindo, D., & Demartines, N. (2004). Classification of surgical complications. *Annals of Surgery*, 240, 205-213.
8. Haxton KJ, & Burt HM. (2009) Polymeric drug delivery of platinum-based anticancer agents. *J Pharm Sci*, 98(7):2299-2316.
9. Sheehy E, Conrad SL, Brigham LE, Luskin R, Weber P, Eakin M, et al.(2003) Estimating the number of potential organ donors in the United States. *N Engl J Med,* 349(7):667-674.

10. Reitz NN, & Callender CO. (1993) Organ donation in the African-American population: a fresh perspective with a simple solution. *J Natl Med Assoc*, 85(5):353-358.
11. Organ Procurement and Transplantation Network (OPTN) and Scientific Registry of Transplant Recipients (SRTR). OPTN / SRTR 2010 Annual Data Report. Rockville, MD: Department of Health and Human Services, Health Resources and Services Administration, Healthcare Systems Bureau, Division of Transplantation, 2010:7.
12. Based on OPTN data of Jan.17th,2012 (http://optn.transplant.hrsa.gov)
13. Harunaga, J. S., & Yamada, K. M. (2011). Cell-matrix adhesions in 3 dimensions. *Journal of the International Society for Matrix Biology*, 30(7-8), 363-368.
14. Rohrmann, D. (2000). The artificial urinary bladder. *World Journal of Urology*, 18, 355-358.
15. Starr, A. (2007). The artificial heart valve. *Nature Medicine*, 13, 1160-1168.
16. Bland (2010). Growing artificial bone. *Materials Today (Kidlington, England)*, 13 (12), p. 10.
17. Luo, Y (2007). Three-dimensional scaffolds" in *Principles of Tissue Engineering (0-12-370615-7, 978-0-12-370615-7)*, (p. 359).
18. Lee CH. (2001). Biomedical applications of collagen. *Int J Pharm,* 221(1-2):1-22.
19. Schmidt CE. (2000). Vascular tissues: natural biomaterials for tissue repair and tissue engineering. *Biomaterials,* 21(22):2215-2231.

20. Putnam AJ. (1996). Tissue engineering using synthetic extracellular matrices. *Nat Med,* 2(7):824-826.
21. Niu CH, & Chiu YY. (1998). FDA perspective on peptide formulation and stability issues. *J Pharm Sci*, 87(11):1331-1334.
22. Mooney DJ, & Organ G. (1994). Design and fabrication of biodegradable polymer devices to engineer tubular tissues. *Cell Transplant,* 3(2):203-210.
23. Stendahl, J. C., & Kaufman, D. B. (2009). Extracellular matrix in pancreatic islets: Relevance to scaffold design and transplantation. *Cell Transplantation*, 18, 1-12.
24. Pollard, T. D., & Earnshaw, W. C. (2008). Cell biology. *Tissue Engineering*, 19, 23-26.
25. Hussey, A. J., Winardi, M. B., & Han. (2009). Seeding of pancreatic islets into prevascularized tissue engineering chambers. *Tissue Engineering*, 15(12), 3823-3833.
26. Merani, S., & Shapiro, J. (2006). Current status of pancreatic islet transplantation. *Clinical Science*, 110, 611-625.
27. Kodama, S., & Kojima, K. (2009). Engineering functional islets from cultured cells. *Tissue Engineering: Part A*, 15, 3321-3329.
28. Beyan, H. (2008). Contemporary endocrinology: Autoimmune diseases in endocrinology. In A. P. Weetman (Ed.). Human Press, NJ. pp. 167-205
29. Pagenkemper, J. J. (2008). Diabetes mellitus. In Nutrition in Kidney Disease. Human Press, NJ. pp. 137-176

30. Wucherpfennig, K. W., & Eisenbarth, G. S. (2001). Type 1 diabetes. *Nature Immunology*, 2, 767-768.
31. Atabek, M. E., & Pirgon, O. (2006). Evidence for an association between type 1 diabetes and premature carotid atherosclerosis in childhood. *Pediatric Cardiology*, 27(4), 428-433.
32. Silink M. (2002). Childhood diabetes: a global perspective. *Horm Res Suppl.* 1:1-5.
33. Onkamo P, & Vaananen S. (1999). Worldwide increase in incidence of Type I diabetes--the analysis of the data on published incidence trends. *Diabetologia*. 42(12):1395-1403
34. Carrasco E, & Perez-Bravo F. (2005). Increasing incidence of type 1 diabetes in population from Santiago of Chile: trends in a period of 18 years (1986-2003). *Diabetes Metab Res Rev*. 18(9): 23-28.
35. Molinari L, & Bagot M. (1994). Epidemiology of IDDM in Switzerland. Increasing incidence rate and rural-urban differences in Swiss men born 1948-1972. *Diabetes Care.* 17(9):955-960.
36. Atkinson, M. A., & Eisenbarth, G. S. (2001). Type 1 diabetes: New perspectives on disease pathogenesis and treatment. *Seminar*, 358(9283), 221-229.
37. Achenbach, P., & Bonifacio, E. (2005). Predicting type 1 diabetes. Current Diabetes Reports, 5(2), 98-103.
38. Gillespie, K. M. (2006). Type 1 diabetes: Pathogenesis and prevention. *CMAJ*, 175(2), 165-170.

39. Longnecker, M. P., & Daniels, J. L. (2001). Environmental contaminants as etiologic factors for diabetes. *Environmental Health Perspectives*, 109(6), 871-876.

40. Bach, J. F. (1987). Mechanisms of autoimmunity in insulin-dependent diabetes mellitus. *Clinical and Experimental Immunology*, 72(1), 1-8.

41. Radha, V (2003). The genetics of diabetes mellitus. *Indian Journal of Medical Research,* 117, p. 225.

42. Sepe, V (2009). Genetics of type 1A diabetes. *The New England Journal of Medicine*, 361 (2), p. 211.

43. Martin, S (2001). Development of type 1 diabetes despite severe hereditary B-lymphocyte deficiency. *The New England Journal of Medicine*, 345 (14), p. 1036.

44. Atkinson, M A (1994). The pathogenesis of insulin-dependent diabetes mellitus. *The New England Journal of Medicine*, 331 (21), p. 1428.

45. Akerblom, H. K., & Knip, M. (1997). Interaction of genetic and environmental factors in the pathogenesis of insulin-dependent diabetes mellitus. *Clinica Chimica Acta*, 257, 143-156.

46. Bliss, M. (1982). The Discovery of Insulin. Chicago: University of Chicago Press.

47. Hahr AJ, & Molitch ME. (2008) Optimizing insulin therapy in patients with type 1 and type 2 diabetes mellitus: optimal dosing and timing in the outpatient setting. *Am J Ther* 15(6):543-550.

48. Saccà, S. (2003). New forms of insulin delivery. *Diabetes, Technology & Therapeutics*, 5(5), 870-875.

49. Doyle, E. A. (2004). A randomized, prospective trial comparing the efficacy of continuous subcutaneous insulin infusion with multiple daily injections using insulin glargine. *Diabetes Care*, 27(7), 1554-1558.
50. Monami, M., & Lamanna, C. (2010). Continuous subcutaneous insulin infusion versus multiple daily insulin injections in type 1 diabetes: A meta-analysis. *Acta Diabetologica*, 47(1), 77-81.
51. Mecklenburg RS, & Benson EA. (1984) Acute complications associated with insulin infusion pump therapy. Report of experience with 161 patients. *JAMA*; 252(23):3265-3269.
52. Nathan DM. (1992) Management of insulin-dependent diabetes mellitus. *Drugs*. 3:39-46.
53. Nathan DM. (1993) Long-term complications of diabetes mellitus. *N Engl J Med.* 328(23):1676-1685.
54. Shyr, Y M (2009). Pancreas Transplantation. *Journal of the Chinese Medical Association*, 72 (1), p. 4.
55. Sutherland, D. R., & Gruessner, A. C. (2007). Long-term results after pancreas transplantation. *Transplantation Proceedings*, 39(7), 2323-2325.
56. Bindi, M. L., & Biancofiore, G. (2007). Early morbidity after pancreas transplantation. *Transplant International*, 18(12), 1356-1360.
57. R. Stratta, N. Hakim & D. Gray (Eds.) Pancreas and islet transplantation. Oxford University Press, Oxford. (2002).

58. Bretzel, R. G. (2003). Pancreatic islet and stem cell transplantation in diabetes mellitus: Results and perspectives. *Tissue Engineering, Stem cells and Gene Therapies*, 534, 69-96.

59. Salvalaggio, R. P., & Davies, D. B. (2006). Outcomes of pancreas transplantation in the United States using cardiac-death donors. *American Journal of Transplantation*, 6(5), 1059-1065.

60. Gruessner, R. G. (1997). Solitary pancreas transplantation for nonuremic patients with labile insulin-dependent diabetes mellitus. *Transplantation*, 64(11), 1572-1577.

61. White, S. A., & Shaw, J. A. (2009). Pancreas transplantation. *Lancet,* 373(9677), 1808-1817.

62. Sutherland, D. E. (2001). Pancreas transplantation for treatment of diabetes mellitus. *World Joural of Surgery*, 25(4), 487-496.

63. Humar, A., & Ramcharan, T. (2004). Technical failures after pancreas transplants: Why grafts fail and the risk factors--a multivariate analysis. *Transplantation*, 78(8), 1188-1192.

64. Sutherland, D. E., & Gruessner, A. C. (1998). Pancreas transplantation: A review. *Transplantation Proceedings*, 30(5), 1940-1943.

65. Stock, P G (2005). Beta cell replacement for Type I diabetes: islet versus solid organ pancreas. *Current Opinion in Organ Transplantation*, 10 (2), 150-154.

66. Maki, T (1995). Novel Delivery of Pancreatic Islet Cells to Treat Insulin-Dependent Diabetes Mellitus. *Clinical Pharmacokinetics*, 28 (6), 471-482.

67. Venturini, Massimo (2005). Technique, complications, and therapeutic efficacy of percutaneous transplantation of human pancreatic islet cells in type 1 diabetes: the role of US. *Radiology* , 234 (2), 617-624.

68. Hatipoglu, B., Benedetti, E. (2005). Islet transplantation: Current status and future directions. *Current Diabetes Reports*, 5(4), 311-316.

69. Bretzel, R. G., & Brandhorst, D. (1999). Improved survival of intraportal pancreatic islet cell allografts in patients with type-1 diabetes mellitus by refined peritransplant management. *Journal of Molecular Medicine*, 77(1), 140-143.

70. Nanji, S. A., & Shapiro, J. (2006). Advances in pancreatic islet transplantation in humans. *Diabetes, Obesity and Metabolism*, 8(1), 15-25.

71. Matsumoto, S (2006). Pancreatic islet transplantation for treating diabetes. *Expert Opinion on Biological Therapy*, 6 (1), 23-37.

72. Hering, B. J. (2005). Single-donor, marginal-dose islet transplantation in patients with type 1 diabetes. *JAMA*, 293(7), 830-835.

73. Deters, N. A., Stokes, R. A., & Gunton, J. E. (2011). Islet transplantation: Factors in short-term islet survival. *Archivum Immunologiae et Therapiae Experimentalis*, 59(6), 421-429.

74. Gaglia, Jason L. (2005). Islet Transplantation: Progress and Challenge. *Archives of Medical Research* (0188-4409), 36 (3), 273-280.

75. Ichii, H., & Ricordi, C. (2009). Current status of islet cell transplantation. *Journal of Hepato-Biliary-Pancreatic Surgery*, 16(2), 101-112.

76. Beck, J., Angus, R., & Madsen, B. (2007). Islet encapsulation: Strategies to enhance islet cell functions. *Tissue Engineering*, 13(3), 589-599.

77. Dall, T. M. (2010). The economic burden of diabetes. *Medical Benefits*, 27(6), 2-4.

78. Jonsson, B (1998). The economic impact of diabetes. *Diabetes Care*, 21 Supplement 3, 7.

79. Cheng, T. O. (2010). Diabetes epidemic in china and its economic impact. *International Journal of Cardiology*, 149, 1-3.

80. Ying, A. K. (2011). Predictors of direct costs of diabetes care in pediatric patients with type 1 diabetes. *Pediatric Diabetes*, 123(3), 177-182.

81. Svendsen, C. Pancreas, *Encyclopedia of Stem Cell Research.* (2008)

82. Rongioletti, F. *Pancreas Disease and Diabetes Mellitus.* (2010).

83. Basturk, O., & Adsay, N. V. Pancreas. *In Essentials of Anatomic Pathology* Springer Science Media. (2011). (pp. 1747-1769).

84. Wellmann., K. F. (1977). *The Diabetic Pancreas.* In B. W. Volk (Ed.), Plenum Press, New York.

85. Mortele, K. J. (2006). Multimodality imaging of pancreatic and biliary congenital anomalies. *Education Exhibit*, 26, 715-731.

86. Islam, S. *The Islets of Langerhans.* Dordrecht, New York. (2010).

87. Freudenrich, C. (2011). Diabetes overview. Retrieved from *The Encyclopedia of Science*

Website: http://health.howstuffworks.com/diseases-conditions/diabetes/diabetes1.htm

88. Jansson, L., & Carlsson, P. O. (2002). Graft vascular function after transplantation of pancreatic islets. *Diabetologia*, 45, 749-763.

89. Pan, X., & Xue, W. O. (2011). Islet graft survival and function: Concomitant culture and transplantation with vascular endothelial cells in diabetic rats. *Transplantation*, 92(11), 1208-1214.

90. Mattsson, G., & Jansson, L. (2002). Decreased vascular density in mouse pancreatic islets after transplantation. *Diabetes*, 51(5), 1362-1366.

91. Garcia-Ocan, A., & Takane, K. K. (2000). Hepatocyte growth factor overexpression in the islet of transgenic mice increases beta cell proliferation, enhances islet mass, and induces mild hypoglycemia. *The Journal of Biological Chemistry*, 275(2), 1226-1232.

92. Miao, G., & Mace, J. (2005). Beneficial effects of nerve growth factor on islet transplantation. *Transplantation Proceedings*, 37, 3490-3492.

93. Liu, J. (2007). Does IGF-I stimulate pancreatic islet cell growth? *Biomedical and Life Sciences*, 48(2-3), 115-125.

94. Li, L (2004). Activin A and Betacellulin: Effect on Regeneration of Pancreatic beta-Cells in Neonatal Streptozotocin-Treated Rats. *Diabetes*, 53 (3), 608.

95. Kaido, Thomas (2004). Regulation of human beta-cell adhesion, motility, and insulin secretion by collagen IV and its receptor alpha1beta1. *The Journal of Biological Chemistry*, 279 (51), 53762-53769.

96. Pileggi, A., Cobianchi, L. (2006). Overcoming the challenges now limiting islet transplantation a sequential, integrated approach. *New York Academy of Sciences*, 1079(1), 383-398.

97. Andersson, A. (2004). Promoting islet cell function after transplantation. *Cell Biochemistry and Biophysics*, 40(3), 55-63.

98. Gibly, R. F., & Graham, J. G. (2011). Advancing islet transplantation: From engraftment to the immune response. *Diabetologia*, 54(10), 2494-2505.

99. Cheng, J., & Raghunath, M. (2011). Matrix components and scaffolds for sustained islet function. *Tissue Engineering Part B: Reviews*, 17(4), 235-247.

100. Hussey, A. J., & Winardi, M. (2009). Seeding of pancreatic islets into prevascularized tissue engineering chambers. *Tissue Engineering Part A*, 15(12), 3823-3833.

101. Salvay, D. M., & Rives, C. B. (2008). Extracellular matrix protein-coated scaffolds promote the reversal of diabetes after extrahepatic islet transplantation. *Transplantation*, 85(10), 1456-1464.

102. Kilkenny, D. M., & Rocheleau, J. V. (2008). Fibroblast growth factor receptor-1 signaling in pancreatic islet β-cells is modulated by the extracellular matrix. *Mol Endocrinol*, 22(1), 196-205.

103. Jiang, F.- M., & Naselli, G. (2002). Distinct distribution of laminin and its integrin receptors in the pancreas. *Journal of Histochemistry & Cytochemistry*, 50(12), 1625-1632.

104. Otonkoski, T., & Banerjee, M. (2008). Unique basement membrane structure of human pancreatic islets: Implications for β-cell growth and differentiation. *Diabetes, Obesity and Metabolism*, 10(s4), 119-127.

105. Kruegel, J., & Miosge, N. (2010). Basement membrane components are key players in specialized extracellular matrices. *Biomedical and Life Sciences*, 67(17), 2879-2895.

106. Meier, J. J., & Butler, A. E. (2010). Increased islet beta cell replication adjacent to intrapancreatic gastrinomas in humans. *Diabetologia*, 49(11), 2689-2696.

107. Virtanen, I., & Banerjee, M. (2008). Blood vessels of human islets of langerhans are surrounded by a double basement membrane. *Diabetologia*, 51(7), 1181-1191.

108. Rosenberg, L (1999). Structural and functional changes resulting from islet isolation lead to islet cell death. *Surgery,* 126 (2), 393.

109. Wang, R. N., & Rosenberg, L. (1999). Maintenance of beta-cell function and survival following islet isolation requires re-establishment of the islet-matrix relationship. *Journal of Endocrinology*, 163(2), 181-190.

110. Peters, M C. (2002). Engineering vascular networks in porous polymer matrices. *Journal of Biomedical Materials Research*, 60 (4), 668.

111. Reparative Medicine: Growing Tissues and Organs. National Institutes of Health Bioengineering Consortium (BECON), Natcher Conference Center, Symposium Report. Bethesda. (2001).

112. Glotzbach, J. P. (2011). Regenerative medicine. *Current Problems in Surgery*, 48(3), 148-212.

113. Kingwell, K (2011). A regenerative medicine. *Nature Reviews. Neuroscience*, 12 (3), 12-17.

114. Muraca, M., Galbiati, G., & Realdi, G. (2007). Regenerative medicine: An insight. *Transplantation Proceedings*, 39, 1995-1998.

115. Andersson, E. R., & Lendahl, U. (2006). Regenerative medicine: A 2009 overview. *Journal of Internal Medicine*, 266, 303-310.

116. Stocum, D (2006). Regenerative Medicine, *Regenerative Biology and Medicine*, 27(9): 337-362.

117. Horch, R. E., & Popescu, L. M. *History of Regenerative Medicine*. (2011). Public Press. MD.

118. Stephen, S. (2007). Regenerative medicine: A growing future. *The Technology Teacher,* 67(8), 10-15.

119. Jannette M, Ray V R, Polymer materials for tissue engineering scaffold. (2005) *Tissue Engineering*, 11(9-10): 1323-1331.

120. Blomeier, H., & Zhang, X. (2006). Polymer scaffolds as synthetic microenvironments for extrahepatic islet transplantation. *Transplantation,* 82(4), 452-459.

121. Principles of Tissue Engineering. In R. Lanza & J. Vacanti (Eds.) (2007).

122. Norman, J. J., & Desai, T. A. (2005). Methods for fabrication of nanoscale topography for tissue engineering scaffolds. *Annals of Biomedical Engineering,* 34(1), 89-101.

123. Chun, S., & Huang, Y. (2008). Adhesive growth of pancreatic islet cells on a polyglycolic acid fibrous scaffold. *Transplantation Proceedings*, 40(5), 1658-1663.

124. Hutmacher, D. W. (2000). Scaffold design and fabrication technologies for engineering tissues — state of the art and future perspectives. *Journal of Biomaterials Science*, 12(1), 107-124.

125. Marcos P, Ruben M B. Scaffold design for tissue engineering. (2008) *Tissue Engineering Part A*. March 2009, 15(3): 569-577.

126. Zhao, M., & Song, C. (2010). The three-dimensional nanofiber scaffold culture condition improves viability and function of islets. *Journal of Biomedical Materials Research Part A*, 94A(3), 667-672.

127. Kin, T., & O'Neil, J. J. (2008). The use of an approved biodegradable polymer scaffold as a solid support system for improvement of islet engraftment. *Artificial Organs*, 32(12), 990-993.

128. Bronzino, J.D. *The Biomedical Engineering Handbook: Biomedical Engineering Fundamentals.* Taylor and Francis Group, Boca Raton, FL (2006).

129. http://www.apjet.com/techsurfacemod.html

130. Alger M. *Polymer Science Dictionary; Second edition,* Chapman & Hill (1997)

131. Kato K, & Kikumura K. (2000) Collagen immobilization onto the surface of artificial hair for improving the tissue adhesion*; J. Adhesion Sci. Technol*., 14(5), 635 –650

132. Mekhail, M., & Wu, Y. (2011). Genipin-cross-linked electrospun collagen fibers. *Journal of Biomaterials Science-Polymer Edition*, 22(17), 2241-2259.

133. Sun, Y., & Mo, X. (2011). Genipin crosslinked gelatin nanofibers for tissue engineering. *Journal of Controlled Release*. 152(s1), 2-6.

134. A. M. Belu, D. J. Graham, D. G. Castner, "Time-of-Flight Secondary Ion Mass Spectrometry: Techniques and Applications for the Characterization of Biomaterial Surfaces", *Biomaterials*, **2003**, *24*, 3635 – 3653.

135. Hussey, A. J., & Winardi, M. (2009). Seeding of pancreatic islets into prevascularized tissue engineering chambers. *Tissue Engineering: Part A*, *15*, 3823-3831.

136. Tambe, N. M. (2011). Surface modification techniques for polymeric biomaterials for use as tissue engineering scaffolds. M.S. Thesis, North Carolina State University, Raleigh, NC, P46-47.

137. He, T. (2011). A study of three dimensional warp knits for novel applications as tissue engineering scaffolds. M.S. Thesis, North Carolina State University, Raleigh, NC, P54.

APPENDICES

APPENDIX A

ANOVA Test for MTT Assay of Collagen Coated 3D 24E6GBXII Scaffold

ni = 4	CO		TG		C1	
	Mean	Sd	Mean	Sd	Mean	Sd
0 Day	0.050	0.005	0.260	0.009	0.240	0.007
3 Day	0.120	0.021	0.440	0.015	0.340	0.019
7 Day	0.110	0.029	0.560	0.025	0.450	0.019
10 Day	0.090	0.022	0.660	0.025	0.550	0.030

ni =4	SST	MST	SSE	MSE	F	p-value
0 Day	0.107	0.054	0.000	0.000	1040.000	0.000
3 Day	0.214	0.107	0.003	0.000	313.145	0.000
7 Day	0.440	0.220	0.005	0.001	361.467	0.000
10 Day	0.731	0.366	0.006	0.001	546.142	0.000

APPENDIX B

ANOVA Test for Insulin Releasing Index (0 Day)

Insulin Releasing Index (0 Day)						
ni = 2	**CO**		**TG**		**C1**	
	Mean	Sd	Mean	Sd	Mean	Sd
0.5hr	1.111	0.231	0.963	0.156	0.823	0.219
1 hr	1.026	0.243	1.256	0.010	1.026	0.259
2 hr	0.860	0.164	1.273	0.232	1.087	0.048
4 hr	0.750	0.218	1.125	0.168	1.025	0.197

ni = 2	**SST**	**MST**	**SSE**	**MSE**	**F**	**p-value**
0.5 hr	0.0830	0.0415	0.1257	0.0419	0.9904	0.4676
1 hr	0.0705	0.0353	0.1262	0.0421	0.8382	0.5139
2 hr	0.1711	0.0856	0.0830	0.0277	3.0918	0.1867
4 hr	0.1508	0.0754	0.1146	0.0382	1.9750	0.2836

APPENDIX C

ANOVA Test for Insulin Releasing Index (3 Day)

Insulin Releasing Index (3 Day)						
ni = 2	**CO**		**TG**		**C1**	
	Mean	Sd	Mean	Sd	Mean	Sd
0.5 hr	0.822	0.051	1.023	0.206	0.891	0.190
1 hr	0.811	0.195	1.339	0.109	1.071	0.251
2 hr	1.430	0.199	1.986	0.112	1.527	0.298
4 hr	0.983	0.084	1.280	0.194	1.144	0.093

ni = 2	**SST**	**MST**	**SSE**	**MSE**	**F**	**p-value**
0.5 hr	0.0417	0.0209	0.0811	0.0270	0.7714	0.5368
1 hr	0.2788	0.1394	0.1129	0.0376	3.7040	0.1548
2 hr	0.3528	0.1764	0.1409	0.0470	3.7547	0.1525
4 hr	0.0884	0.0442	0.0533	0.0178	2.4864	0.2309

APPENDIX D

ANOVA Test for Insulin Releasing Index (7 Day)

Insulin Releasing Index (7 Day)						
ni = 2	**CO**		**TG**		**C1**	
	Mean	Sd	Mean	Sd	Mean	Sd
0.5 hr	4.729	0.316	5.523	0.178	5.635	0.283
1 hr	3.897	0.211	6.988	0.236	5.041	0.319
2 hr	2.425	0.255	6.480	0.317	5.225	0.199
4 hr	2.154	0.253	4.118	0.243	3.154	0.188

ni = 2	**SST**	**MST**	**SSE**	**MSE**	**F**	**p-value**
0.5 hr	0.9759	0.4879	0.2116	0.0705	6.9169	0.0752
1 hr	9.7692	4.8846	0.2020	0.0673	72.5516	0.0029
2 hr	17.2387	8.6194	0.2051	0.0684	126.0661	0.0013
4 hr	3.8577	1.9289	0.1584	0.0528	36.5311	0.0078

APPENDIX E

ANOVA Test for Insulin Releasing Index (10 Day)

Insulin Releasing Index (10 Day)						
ni = 2	**CO**		**TG**		**C1**	
	Mean	Sd	Mean	Sd	Mean	Sd
0.5 hr	0.534	0.350	5.585	0.248	2.606	0.204
1 hr	1.800	0.242	6.402	0.345	3.836	0.327
2 hr	2.838	0.371	7.752	0.203	4.661	0.357
4 hr	0.641	0.306	4.227	0.498	1.601	0.278

ni = 2	**SST**	**MST**	**SSE**	**MSE**	**F**	**p-value**
0.5 hr	25.7868	12.8934	0.2256	0.0752	171.4397	0.0008
1 hr	21.2720	10.6360	0.2845	0.0948	112.1478	0.0015
2 hr	24.6833	12.3417	0.3063	0.1021	120.8786	0.0014
4 hr	13.7846	6.8923	0.4189	0.1396	49.3571	0.0051